HEAT TRANSFER ENHANCEMENT IN A RECTANGULAR CHANNEL USING VORTEX GENERATOR IN A LAMINAR FLOW

by

NINAD C. MANIAR

Presented to the Faculty of the Graduate School of

The University of Texas at Arlington in Partial Fulfillment

of the Requirements

for the Degree of

MASTER OF SCIENCE IN MECHANICAL ENGINEERING

THE UNIVERSITY OF TEXAS AT ARLINGTON

December 2012

Acknowledgements

I am thankful to my research advisor, Dr. Brian Dennis, for his guidance and support during the last few years that have helped me grow both personally and academically. This thesis would not have been possible without him. I am privileged to be working under his guidance and have learned a great deal from him. I am grateful to all my professors for helping me during difficult times with my Master's program. I am grateful to Dr. Kent Lawrence and Dr. Bo Ping Wang for serving as committee members and also for being great advisors. I am also grateful to Debi Barton for helping me throughout my Master's degree with her immense experience in administration. I am thankful to Barbara Sellers and Virginia Marzoni for their care and biased support towards me.

I am thankful to Deval Pandya and Abhijit Paranjape who have been wonderful and supportive friends and colleagues. They have helped me at the time of my need. I am also thankful to all my friends, new and old, for being there for me.

I would like to specially thank Gunjan Maniar, my brother, for his boundless support throughout my life. And lastly, I am indebted to my parents, Mr. Chandresh Maniar and Mrs. Pratima Maniar, for their unconditional love and belief in me.

November 26, 2012

Abstract

HEAT TRANSFER ENHANCEMENT IN A RECTANGULAR CHANNEL

USING VORTEX GENERATOR IN A

LAMINAR FLOW

Ninad C. Maniar, M.S.

The University of Texas at Arlington, 2012

Supervising Professor: Brian H. Dennis

Enhancement of heat transfer through various means has been an intense area of research for many years. There are numerous applications where high performance heat exchange is desired. The cooling of electronics, such as microprocessors, is one example. The recent rise in the studies of heat exchange enhancement techniques has also lead to efficient and compact heat exchangers. This research involves the numerical analysis of heat exchange enhancement in a rectangular channel using different types of longitudinal vortex generators (LVG) for a laminar flow. A computational fluid dynamics software package was used to compute the 3-D steady viscous flows with heat transfer. The effects of Reynolds number ranging from 500 to 1000 (laminar flow) are shown from different attack angles of the vortex generators (30˚ and 45˚). Three different types of vortex generators are studied: a delta wing with finite thickness, a trapezoidal delta wing, and a delta winglet pair (also called half delta wing) for a common flow down configuration. The Nusselt number ($\overline{\mathrm{Nu}}$) is computed and compared with the Nusselt number ($\overline{\mathrm{Nu}_0}$) without the LVG's. The results show that the LVG's effectively enhances the heat transfer in the rectangular channel. In addition, the impact of the LVG's drag and

the resulting pressure drop across the channel was quantified. The Darcy's friction factor (f) was computed and compared with the friction factor without LVG's (f_0). For each case the performance evaluation parameter ($(\overline{Nu}/\overline{Nu_0})$ / (f/f_0)) was computed to gauge the overall efficiency of the configuration. Results are discussed and recommendations for future investigations are given.

Table of Contents

List of Illustrations

List of Tables

Chapter 1

Introduction

1.1 Background

Increasing demands on the performance of heat exchangers used in power systems, automotive industry, electric circuit in electronic chip cooling, air conditioning and refrigerant applications, internal cooling of gas turbine blades and aerospace industry for reasons of compactness, manufacturing cost effectiveness and higher efficiency lead to use of heat transfer enhancement techniques. Heat transfer enhancement is usually required in heat exchangers. Various heat transfer enhancement techniques are used such as fins, ribs, dimpled surfaces, and protruding surfaces that generate vortices in a heat exchanger.

Heat sinks and heat exchangers are used in many applications today and the most common material used is aluminum because of its high thermal conductivity (205 W/m·K), low maintenance and production cost, and less weight. Copper is also used at times because of its very high conductivity (400 W/m·K), but it is not commonly used because it is heavy and costly. At times, diamond is also used for heat exchange enhancement since it has thermal conductivity of 2000 W/m·K; however, it is not commonly used unless called for because it is very expensive. Diamond is used in high powered integrated circuits. For higher performance, heat exchangers require more space and surface area, less weight and low cost. Hence, at times heat exchangers are made of aluminum and copper alloys because of their advantages. To improve performance, heat exchangers should have a large surface area since the heat transfer takes place on the surface. Various techniques are used to enhance heat transfer. In this study, aluminum is used as the material for the rectangular channel walls.

There are two different methods for heat exchange enhancement: active vortex method and passive vortex method [28]. The active vortex method is used to actively control the secondary flow and pressure drop so as to meet the required heat transfer rates even at the cost of increased pumping power. There is little known use of this method in heat exchangers since the operating cost is very high. A few examples of active vortex method are the use of jets at different angles from the heat transfer surface into the boundary layer [21], and the generation of a secondary flow through acoustic excitation [34], and Electrohydrodynamics (EHD) which is the process of producing an electric field to create electric body force in the flow [19]. Using longitudinal or latitudinal vortex generators for heat exchange enhancement is known as the passive vortex method. Delta wing, rectangular wing, delta winglet, rectangular winglet, trapezoidal delta wing, dimpled surfaces, ribs, and fins all are types of vortex generators. A great deal of research has been done using this method since it is efficient and has low maintenance and operating cost in heat exchangers. In this study, the use of passive vortex devices and its extensive use in heat exchangers for heat transfer enhancement is described.

There are two types of vortex generators; transverse vortex generators (TVG's) (or latitudinal vortex generators) and longitudinal vortex generators (LVG's).The rotational direction of the transverse vortex generator to the main flow direction is normal and the flow is two-dimensional, while the longitudinal vortex generators have their rotating axes parallel to the main flow and the flow is three-dimensional. Vortex generators are usually included in the flow on a plate or a channel at an angle of attack, β by either protruding wings or winglets, or by punching holes or dimples on the surface. It is also known that it is impossible to produce pure longitudinal vortices, since transverse vortices are always generated by the vortex generators. The angle of attack determines the dominance of one over the other. When the attack angle is finitely small, mainly longitudinal vortices are

generated. The higher the angle of attack the more transverse vortices are generated. Only transverse vortices are generated when the angle of attack is 90˚.

The laminar sublayer (or the viscous sublayer) is a region of turbulent flow nearer to the no-slip boundary region where the flow is laminar. The velocity decreases towards the no slip boundary region thus decreasing the Reynolds number. Both conductive and convective heat transfer occurs in the region outside the laminar sublayer while the region inside the sublayer is only conductive; hence, the thermal resistance is mainly enclosed in the viscous sublayer. The transverse vortex generators do not disturb the viscous sublayer while the longitudinal vortex generators disturb the viscous sublayer in the direction of the flow, enhancing the heat transfer. Another advantage of longitudinal vortex generators over transverse vortex generators is that they show low flow loss ([8] and [12]). But, it does not mean that only longitudinal vortices at a very low attack angle (β = 2˚ -10˚) are desirable; at times higher attack angles (β = 15˚-60˚) are required for excessive heat transfer. In this study angles of attack, β of 30˚ and 45˚ are used.

Winglet pairs are placed in two configurations: common flow down and common flow up. In this study the winglet pairs, rectangular or delta, are placed at a certain angle of attack (β = 30˚ and 45˚) creating counter rotating pairs of vortices behind the LVG's in the direction of the flow. Common flow down (CFD) configuration of a winglet pair is demonstrated when the transverse distance between the leading edges is less than that of the trailing edges. For CFD, the left winglet forms vortices rotating in a clockwise direction while the right winglet forms vortices rotating in a counterclockwise direction as shown in Figure 1-1 (a). These vortices create the down wash flow towards the lower channel wall while the up wash flow is away from the wall which is found in the outside region of the vortices. Along the downstream direction, the secondary velocity vectors

decreases while the distance between the vortex cores increases. Thinning of the thermal boundary layer thus occurs in between the two vortices.

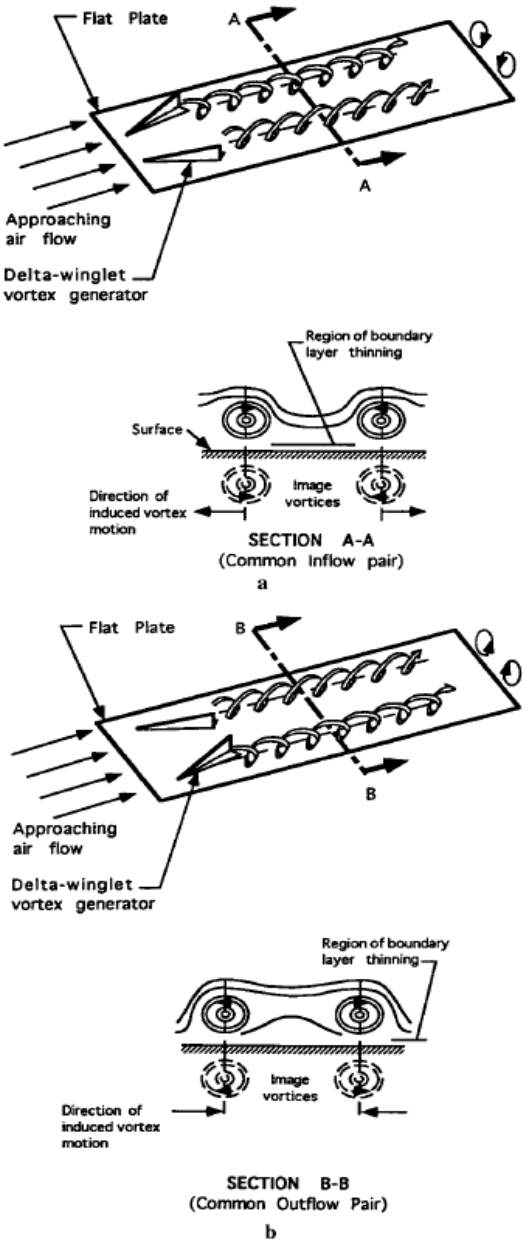

Figure 1-1 Direction of vortices generated in (a) common flow down, (b) common flow up configuration [12]

In common flow up (CFU) configuration, the transverse distance between the leading edges of the winglet pair is more than the distance between the trailing edge; hence, the left winglet forms vortices rotating in a counterclockwise direction while the right winglet forms vortices rotating in a clockwise direction as shown in Figure 1-1 (b). The vortices create the up wash flow between the vortices while the down wash flow on the outer region of vortices towards the lower channel wall. Also, the distance between the vortex cores decreases, hence, the interaction between the counter rotating vortex pair increases considerably. It is also observed that the core of the vortices in CFU gradually moves from the lower wall to upper wall as the flow moves downstream. The thinning of the thermal boundary layer is on the outer region of the vortices.

Figure 1-2 shows the flow pattern over the top of a trapezoidal delta wing at an angle of attack (shown as α in the Figure 1-2). The figure shows that the flow creates two prominent vortex patterns which are created since the pressure on the bottom surface of the wing is higher than the pressure at the top surface. Hence, the flow adjacent to the leading edge gives rise to curls around the leading edge from bottom to top. This curl forms the main vortex also called the primary vortex and, if the leading edge is sharp, it runs throughout the length of the wing, hence separating the flow. The primary separation line, S_1 separates at the leading edge loops above the wing and reattaches itself along the primary attachment line, A_1. Sometimes, an induced vortex or secondary vortex is formed underneath the primary vortex, with its own separation line, S_2, and its own reattachment line, A_2.

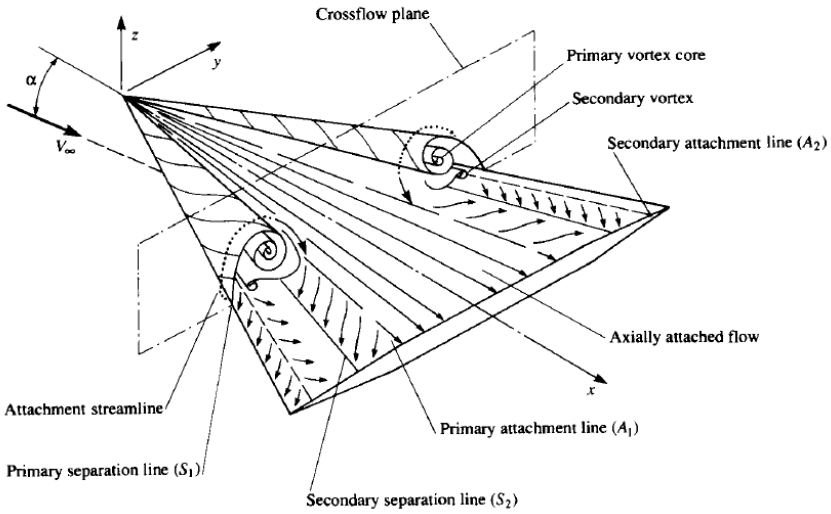

Figure 1-2 Flow over a trapezoidal delta wing showing the different vortices generated [1]

Channels with LVG's result in a higher Nusselt number but they also create large pressure drops, hence analytical evaluation is conducted under these constraints: identical mass flow rate, identical pressure drop, identical pumping power, and performance evaluation parameter.

Besides the use of vortex generators (ribs, fins, and dimples surfaces) for heat exchange enhancement they are also used because they provide larger heat transfer surface and also assist in achieving higher heat transfer coefficient by increasing disturbances (wakes) or by decreasing the thermal boundary layer. Hence, many flat plate heat exchangers use ribs and fins that are wavy, louvered, or slotted. The flow is vigorously disturbed by the vortex generation from wings or winglets or punched holes. Vortex generators not only disturb the flow, disrupting the growth of the boundary layer, but also cause the fluid to swirl (air, water, and usually low viscous fluid) which, in turn, causes extreme exchange of wall and core fluid leading to heat exchange enhancement.

A major disadvantage of protruding vortex generators like wings and winglets is that it produces parasitic drag which leads to pressure drop across the flow. There are basically three types of parasitic drag: form drag, interference drag, and skin friction drag. Form drag and skin friction drag affect the vortex generators primarily. Form drag appears because of the form of the body in the path of the flow. Bodies with greater cross section will induce greater form drag. Streamlined bodies will induce minimum drag. Skin friction drag appears because of the friction of the fluid against the body in the path of the flow. It arises from the interaction between the fluid and the body and depends on the surface of the body in contact with the fluid. Dimpled surfaces only exhibit skin friction drag and no form drag and, hence, they are usually preferred over the conventional LVG's. Low maintenance and manufacturing cost, along with a few constraints such as not removing material from the surface and using smaller surface area for same heat transfer enhancement, tend to be more favorable towards using LVG's.

1.2 Literature Review

Heat exchange enhancement by swirl or vortex generation is an important mechanism in steady flow. The flow must be steady in order to separate the swirl effect from the destabilization effect of the vortices. As mentioned, due to flow separation, the vortices are generated. The first use of longitudinal vortex was mentioned by Schuauer and Spangenberg [22] and since then research on LVG's has increased. Tiggelback et al. [25] established that in a rectangular channel, a pair of delta winglet performs better than a pair of rectangular winglets at a higher angle of attack and Reynolds number. Biswas et al. [2] showed that delta winglet pair has less flow loss than single wing and can eliminate zones of poor heat transfer. They also discuss the different types of vortices generated in the flow. Feibig et al. [7] showed the performance of delta pair wings and winglets and

rectangular wings and winglets in a flat plate and channel flow. They showed that heat transfer enhancement increases with increasing Reynolds number. Sohankar [23] showed that as the Reynolds number increases, the vortex strength increases. Gentry and Jacobi ([9] and [10]) showed heat transfer enhancement characteristics of delta wing vortex generators in a flat plate channel flow. Results showed that the average heat is enhanced by 50-60% for a laminar flow. Jacobi and Shah [12] showed that LVG's generate large scale longitudinal vortices and, hence, enhance heat transfer. They also reviewed the active and passive methods for heat exchange enhancement in the past few years. Tian et al. [24] compared delta winglet pair with rectangular winglet pair (RWP) for common flow down and common flow up configuration and presented that delta winglet pair (DWP) in a common flow down configuration is more efficient than any other configuration. They also discussed that the Nusselt number for rectangular winglet pairs affects more than delta winglet pairs for different configurations. They also showed that the friction factor for RWP is higher than that of DWP. Wu et al. [30] numerically studied the effect of punched delta winglet pairs at different attack angles in a rectangular channel. They showed the average heat transfer of both sides of the channel increases with an increase in Reynolds number and angle of attack. They concluded that the thickness for a RWP with or without punched holes, shows a lower average Nusselt number than in the case of zero thickness. They showed that the higher Nusselt number is found in a rectangular channel with holes than without but the friction factor is higher, too. They also showed that an attack angle of 45˚ is more effective than 15˚, 30˚, 60˚, and 90˚ and the pressure drop also increases with the increase in angle of attack. Another study, both experimental and numerical, by Wu et al. [29] shows that heat transfer enhancement in a rectangular channel decreases with the increase of LVG's location from the channel inlet and with the decrease in transverse space between the LVG pair.

They also showed that with an increase in area, both heat transfer enhancement and pressure loss will increase, at a fixed area of LVG. Properly increasing the length and decreasing the height is a good idea to get more heat transfer enhancement and to prevent significant flow loss. It was concluded that DWP, which is half the channel height, gives better results than DWP with height equal to channel height. Hiravennavar et al. [11] proved that a DWP of finite thickness performs better than a DWP with zero thickness. Ferrouillat et al. [6] showed that the delta winglet pair and rectangular winglet pair of finite thickness both help in heat transfer but the delta winglet pair is more efficient. They also showed that the distance between two vortex generator rows should be seven to ten times the channel height. Wang et al. [27] experimentally showed that LVG's on both sides is better than on just one side in a rectangular channel. Deb et al. [5] showed their computational results are in agreement with the experimental results for heat transfer in laminar and turbulent flows in a rectangular channel using DWP. Also, turbulent flow uses less computational time and storage than low Re near wall models. Yang et al. [31] accurately predicted the vortex characteristics and presented results that were reasonably close to the experimental results for a pair of DWP in a rectangular channel for a turbulent flow. Kim and Patel [15] conducted experimental and numerical studies of the interaction between the vortices and the turbulent boundary layer generated in the duct having flat plates or curved wall boundary layers. They also showed that the circulation of both CFD and CFU vortices increases with downstream flow in a concave channel while it is not the same on a flat plate or convex surface. Zhu et al. [33] showed that a combination of LVG's on one wall and roughness elements on the other wall shows better heat transfer enhancement for turbulent flows. Torii et al. [26] showed that a common flow up configuration is more efficient than a common flow down configuration in a fin-tube heat exchanger. In a finned oval tube type heat exchanger,

Chen et al. [3] concluded that performance enhancement by punched winglets increased with increasing Re while performance of the channel is less dependent with an increase in the number of punched winglets. Chen et al. [3] concluded that a staggered arrangement is more effective than in line arrangement of punched DWP at low Re for a finned oval tube heat exchanger. In a slit fin and tube heat exchanger, Li et al. [16] showed that higher heat transfer performance is obtained with moderate pressure drop. Mahmood et al. ([17] and [18]) experimentally showed the flow of staggered arrays of dimples in a channel and the influence of aspect ratio, temperature ratio, and Reynolds number ranging from 600 to 61500 for heat transfer enhancement. An active vortex method of using jets was discussed by Zhang et al. [32], and the method has been experimentally studied as a means of active boundary layer control ([4] and [13]). The jets are generally circular in shape and are injected with a particular skew angle, pitch, and velocity equal to the free stream velocity ([4] and [13]). Another active vortex method, called EHD, relies on an externally provided electric field to produce an electric body force closer to the heat transfer surface while directly increasing the heat transfer coefficients and, thus, increasing the performance of the system ([19] and [20]). Zohir [34] studied the influence of pulsation on heat transfer enhancement and concluded that heat transfer enhancement for counter flow is much higher than that of a parallel flow in concentric double pipe heat exchangers.

In this study, the cross section of the rectangular channel is 0.16 x 0.04 m and the channel length is 0.4 m. The inlet section is the same length as that of the middle channel, that is, 0.4 m while the outlet section is 0.6 m. The reason for the inlet length is so that the flow can be fully developed and so that the velocity profile is parabolic in laminar flow. This means that the fluid velocity is zero at the surface since it has the no slip condition while the maximum velocity is formed at the center. It is easier to work with

average velocity, V_{avg}, as the velocity remains constant in an incompressible flow when the cross sectional area of the pipe does not change. Hence, sacrificing marginal accuracy is justified over the convenience of constant properties. The flow is laminar and the Reynolds numbers are chosen as 500, 750 and 1000. The maximum length of the wings or winglets is 0.04 m while the chord length is 0.034641 m. The transverse distance between the DWP's is 0.01 m and the distance of the LVG's from the middle section is 0.08 m (0.48 m from the inlet section).

Chapter 2

Computational Fluid Dynamics

2.1 Introduction

Computational Fluid Dynamics also generally called CFD is an important branch of fluid mechanics and it uses numerical methods and algorithms to analyze and solve fluid flow problems. It has become popular since the previous methods, experimental and theoretical are either very expensive, time consuming, or involve too much labor. In CFD, computers are used to solve the algorithms that define and analyze the fluid flow. Due to the increase in the computational capabilities over time and better numerical solving methods, most experimental and theoretical work has been done using CFD. CFD is not only cost effective but it helps one analyze and simulate complex geometries, heat transfer, and shock waves in a fluid flow. It also helps solve partial differential equations (PDE) of any order in a fluid flow. CFD mainly helps analyze the internal or external fluid flow. The use of CFD has become increasingly popular in branches of engineering such as Aerospace to study the interaction of the propellers or rotors with aircraft fuselage, Mechanical to obtain temperature distribution of a mixing manifold, Bio-medical engineering to study the respiratory and circulatory systems. There are a few simple generic steps that must be followed for CFD analysis.

2.1.1 Pre-Processing and Geometry Modeling

The first step to any problem is, knowing the problem. A problem well stated is a problem well resolved Data already known is used in this process. Hence, the type and size of the geometry is already known. Geometry modeling tools such as Creo Parametric, AutoCAD, Pro/ENGINEER, and SolidWorks are used to create and model the geometry. The problem has an objective which helps specify the objective functions

and apply the given constraints to a fluid flow. Creo Parametric 2.0 was used in this study to model the geometry.

2.1.2 Meshing

Meshing (also called grid generation) is the process of splitting flow domains into sub domains which are primarily composed of triangles or quadrilaterals for 2D geometry or tetrahedral or hexahedra in 3D geometry. Governing equations are discretized and solved in every single sub domain. The sub domains are called cells or elements. Combined, they are collectively called mesh. Grids are normally classified as structured, unstructured, or mixed. Grids are generated in Pointwise, Gambit, or ANSYS Workbench. In this study ANSYS Workbench 12.0.1 was used to mesh the geometry that was imported from Creo Parametric 2.0.

The Finite Volume Method (FVM) is the most common approach used for obtaining CFD simulation. As the name suggests, the governing equations are solved over discrete control volumes. This method reforms the governing partial differential equations, especially the Navier-Stokes equation in a conservative form and then discretizes the new equation. The Finite Element Method (FEM) is commonly used in the structural analysis of solids. In FEM, the problem is divided into very small elements which are related to one another. FEM is more stable than FVM and, at times, can require more memory than FVM. The Finite Differential Method (FDM) is a method for approximating solutions to differential equations.

2.1.3 Setup

Boundary conditions at inlet, outlet, and across the whole fluid flow along with viscosity, property of the fluid, and operating conditions are the various parameters that

need to be defined once the meshing is completed. In this study FLUENT 12.0.16, the most commonly used commercial software, is used to set up and solve the flow. The choice of algorithms, models, solution methods, and accuracy convergence are also chosen to solve the flow.

2.1.4 Post-Processing

The desired results are processed according to the requirement of the problem,. Various properties such as temperature, velocity, Mach number, and pressure are extracted from the results. At times the entire process is repeated to insure better results by controlling the under relaxation factor and improving the mesh quality.

2.2 Governing Equations

Navier-Stokes equation plays a very important role for simulation of CFD problems. This comes from applying Newton's second law to fluid motion. Partial differential equations define mass, momentum, and energy flow conservation.

In this study, the flow in the rectangular channel is considered laminar, incompressible, and steady state. The Navier-Stokes equation is shown in the simplest form. The following assumptions were made,

1. It is a steady flow. Thus, this study does not depend on the time.
2. The fluid has constant density and viscosity which means it is incompressible ρ = constant. Thus, the thermal changes that occur in the fluid because of constant density are neglected in this study.
3. The only velocity component at inlet is in the direction of the flow, u = V. Thus, v = w = 0.
4. The inlet in the rectangular channel is fully developed, thus $\frac{\partial u}{\partial z} = 0$,

5. Gravity is neglected in this study and the thermal changes due to gravity are very small which are also neglected, and
6. The wall has non slip conditions. The velocity is zero at contact with the wall, thus u = 0 at the wall.

The following scales and non-dimensional variables are used,

$$x^* = \frac{x}{L},$$

$$u^* = \frac{u}{V},$$

$$P^* = \frac{p}{\rho V^2},$$

$$\frac{\partial}{\partial x^*} = \frac{1}{L}\frac{\partial}{\partial x^*},$$

$$Re = \frac{VL}{\vartheta} = \frac{V^2/L}{\vartheta V/L^2},$$

$$T^* = \frac{T - T_{in}}{T_w - T_{in}}$$

The continuity equation in a non-dimensional form for a steady state flow is given by,

$$\frac{\partial u^*}{\partial x^*} + \frac{\partial v^*}{\partial y^*} + \frac{\partial w^*}{\partial z^*} = 0$$

The momentum equation in a non-dimensional form for a steady state flow is given by,

$$u^*\frac{\partial u^*}{\partial x^*} + v^*\frac{\partial u^*}{\partial y^*} + w^*\frac{\partial u^*}{\partial z^*} + \frac{\partial P^*}{\partial x^*} = \frac{1}{Re}\left(\frac{\partial^2 u^*}{\partial x^{*2}} + \frac{\partial^2 u^*}{\partial y^{*2}} + \frac{\partial^2 u^*}{\partial z^{*2}}\right)$$

$$u^*\frac{\partial v^*}{\partial x^*} + v^*\frac{\partial v^*}{\partial y^*} + w^*\frac{\partial v^*}{\partial z^*} + \frac{\partial P^*}{\partial y^*} = \frac{1}{Re}\left(\frac{\partial^2 v^*}{\partial x^{*2}} + \frac{\partial^2 v^*}{\partial y^{*2}} + \frac{\partial^2 v^*}{\partial z^{*2}}\right)$$

$$u^*\frac{\partial w^*}{\partial x^*} + v^*\frac{\partial w^*}{\partial y^*} + w^*\frac{\partial w^*}{\partial z^*} + \frac{\partial P^*}{\partial z^*} = \frac{1}{Re}\left(\frac{\partial^2 w^*}{\partial x^{*2}} + \frac{\partial^2 w^*}{\partial y^{*2}} + \frac{\partial^2 w^*}{\partial z^{*2}}\right)$$

The energy equation in a non-dimensional form for a steady state flow is given by,

$$\frac{\partial(u^*T^*)}{\partial x^*}+\frac{\partial(v^*T^*)}{\partial y^*}+\frac{\partial(w^*T^*)}{\partial z^*}=\frac{1}{Re\,Pr}\left[\frac{\partial^2T^*}{\partial x^{*2}}+\frac{\partial^2T^*}{\partial y^{*2}}+\frac{\partial^2T^*}{\partial z^{*2}}\right]$$

Chapter 3

Numerical Description

3.1 Introduction

In this chapter, a complete description of the numerical simulation is provided. Geometric modeling, computational grid, and setup for this model are discussed. The flow is laminar and the velocity of the flow is calculated as,

$$\mathrm{Re} = \frac{\rho V H_d}{\mu},$$

where, Re = Reynolds number, (dimensionless)

ρ = density of the fluid, (kg/m^3)

V = mean velocity of fluid flow, (m/s)

H_d = characteristic length or hydraulic diameter, (m)

μ = dynamic viscosity of the fluid, (kg / (m·s))

In this case, since the flow is through a rectangular channel, the hydraulic diameter is taken as

$$H_d = \frac{4 * \text{Area of the rectangular cross section}}{\text{Perimeter of the rectangular cross section}}$$

$$H_d = \frac{4 * B * H}{2(B + H)}$$

$$H_d = 64 \text{ mm or } 0.064 \text{ m}$$

Density of the air is 1.225 kg/m^3 and the dynamic viscosity of air is 1.7894 * 10^{-5} kg / (m·s).

Prandtl number is the ratio of kinematic viscosity to thermal diffusivity and it is a dimensionless number. Higher Prandtl number means, the convective heat transfer is strong. The Prandtl number for air in this study is taken as 0.7

$$\mathrm{Pr} = \frac{\vartheta}{\alpha}$$

where, ϑ = kinematic viscosity of the fluid = μ/ρ, (m^2/s)

α = thermal diffusivity of the fluid = $K/\rho C_p$, (m^2/s)

K = thermal conductivity of the fluid, (W / (m·K))

C_p = specific heat of the fluid, (J / (kg·K))

Nusselt number is the ratio of convective heat transfer coefficient to the conductive heat transfer coefficient. It is a dimensionless number. Nusselt Number is close to one when the magnitude of convection and conduction are similar and it is found in a laminar flow. For fully developed internal laminar flow, the Nusselt number is a constant value. The values depend on the hydraulic diameter.

$$\mathrm{Nu} = \frac{\mathrm{h} \cdot \mathrm{H_d}}{\mathrm{K}}$$

where, h = heat transfer coefficient, (W / (m^2·K))

H_d = hydraulic diameter, (m)

The average surface Nusselt number is the surface integral of Nusselt number over a given surface and is denoted as $\overline{Nu}$.

The heat transfer coefficient is used to calculate the convective heat transfer.

$$\mathrm{h} = \frac{\mathrm{Q}}{\mathrm{A} \cdot \Delta \mathrm{T}}$$

where, Q = heat transfer capacity, (W)

A = heat transfer surface area, (m^2)

ΔT = log mean temperature difference, (K)

The log mean temperature difference (LMTD) is the logarithmic average between the hot and cold streams at inlet and outlet of the heat exchanger. Larger LMTD signifies higher heat transfer.

$$\Delta T = \frac{(T_w - T_{in}) - (T_w - T_{out})}{\ln[(T_w - T_{in})/(T_w - T_{out})]}$$

where, T_w = wall temperature, (K)

T_{in} = temperature at inlet, (K)

T_{out} = temperature at outlet, (K)

Darcy's friction factor is a dimensionless quantity which is used to describe the friction losses in a pipe or channel and is given by

$$f = \frac{2\Delta p \cdot H_d}{L \cdot \rho \cdot V^2}$$

Where, f = Darcy's friction factor,

Δp = pressure loss, (Pa)

H_d = hydraulic diameter, (m)

L = length of the channel, (m)

ρ = density of the fluid, (kg / m^3)

V = mean velocity of fluid flow, (m/s)

The Performance Evaluation Parameter (PEP) is the ratio of the average surface Nusselt number ratio to the Friction factor ratio and it is also a dimensionless quantity.

$$PEP = \frac{\overline{Nu}/\overline{Nu_0}}{f/f_0},$$

The inlet section, heated section and outlet section is shown Figure 3-1 though the heated section isn't very clearly visible. The bottom of the middle section along with vortex generator is the heated section. The rest of the surfaces of the channel are the walls which are adiabatic in nature at 300 K and where no slip boundary condition is applied. The applied boundary conditions are shown below.

The inlet boundary condition is u = V, v = 0, w = 0, T = T_{in} = 300 K,

The outlet boundary condition is $\frac{\partial u}{\partial x} = \frac{\partial v}{\partial y} = \frac{\partial w}{\partial z} = \frac{\partial T}{\partial x} = 0$,

On the lower wall, u = v = w = 0, and T = T_w = 400 K,

Other boundary conditions are, v = 0 and w = 0, thus,

$$\frac{\partial u}{\partial y} = \frac{\partial w}{\partial y} = \frac{\partial T}{\partial y} = \frac{\partial u}{\partial z} = \frac{\partial y}{\partial z} = \frac{\partial T}{\partial z} = 0$$

The surface of the LVG has a no slip boundary conditions for the velocities. The temperature is constant and equal to T_w = 400 K.

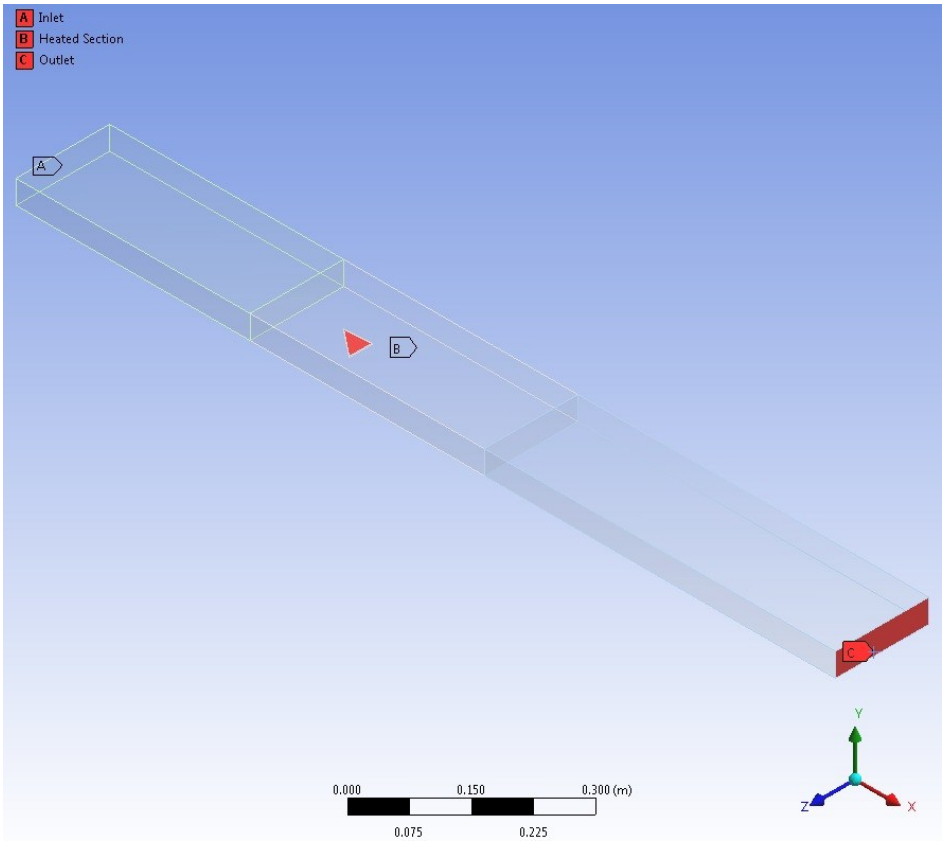

Figure 3-1 Isometric view of the entire channel, showing inlet section, heated section, and outlet section.

3.2 Geometric Model

The rectangular channel has a cross-section of 0.16 x 0.04 m; the length is 0.4 m. The cross-section of the inlet section is 0.16 x 0.04 m and the length is equal to that of the rectangular channel which is 0.4 m. The inlet section is built so that the flow is fully developed and can have a parabolic laminar flow. The cross section of the outlet section is 0.16 x 0.040 m and the length is 0.6 m. The streamwise coordinate of the LVG's from the end of the inlet section is 0.08 m. The chord length of the wing or winglet is 0.034641 m. The flow in the channel is laminar, and Re is chosen as 500, 750 and 1000. Shown in Figure 3-2 is the isometric view of the channel along with the inlet and outlet section.

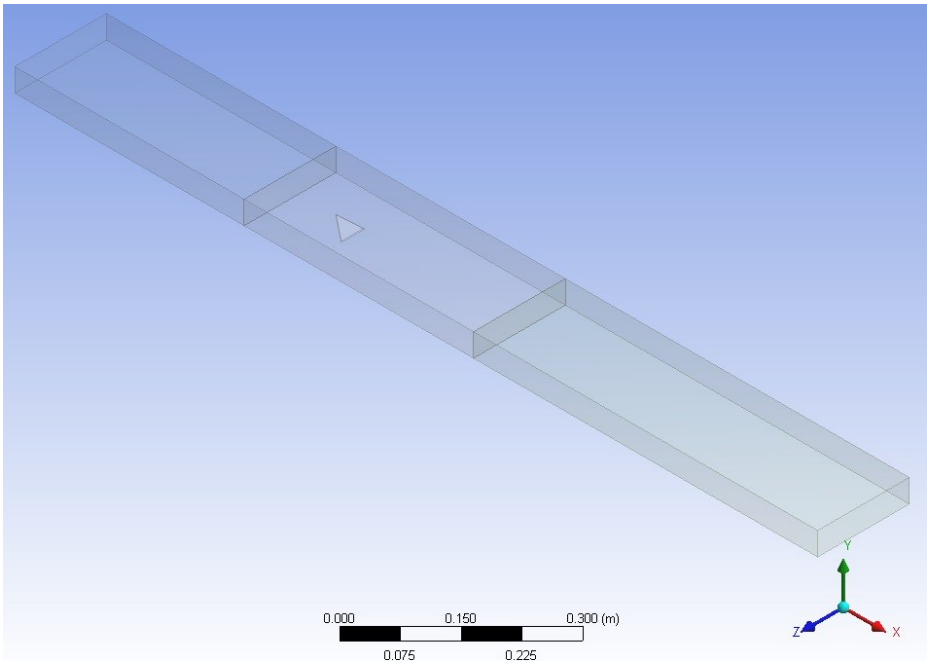

Figure 3-2 Isometric view of the entire channel showing the inlet section, rectangular middle section with the vortex generator and outlet section

3.2.1 Delta Wing

The delta wing is shown in Figure 3-3 and Figure 3-4. The geometry is that of a delta wedge with a thickness of 0.001 m and all the sides of the delta wing are equal.

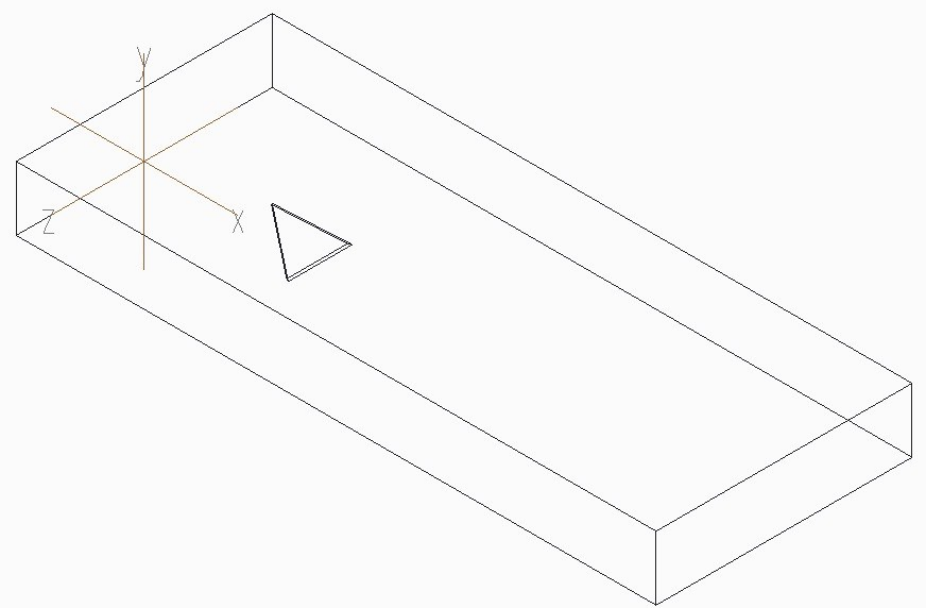

Figure 3-3 Isometric view of the delta wing with attack angle, β = 30˚

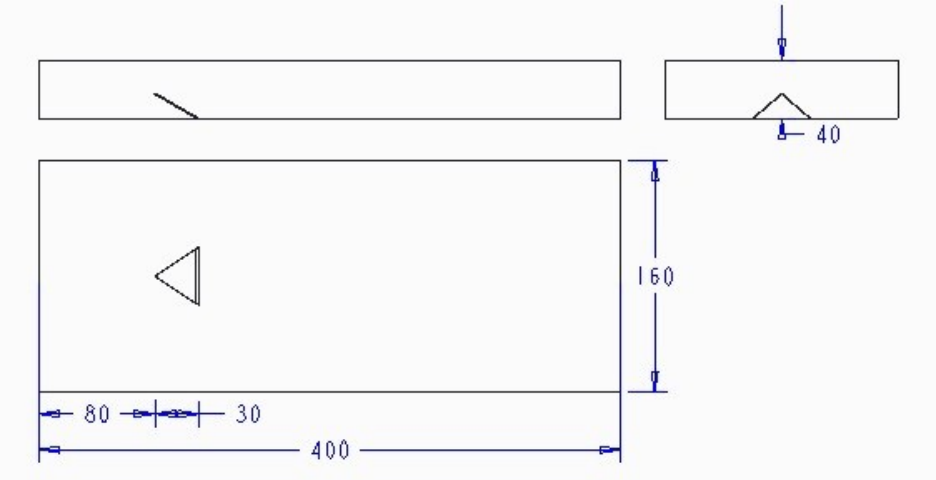

Figure 3-4 Orthographic view of the delta wing with β = 30˚ (dimension in mm)

3.2.2 Trapezoidal Delta Wing

The trapezoidal delta wing is shown in Figure 1-2 and Figure 3-5 while the orthographic view is shown below in Figure 3-6. The base of the wing has a thickness of 0.001 m and sides of 0.04 m and 0.02 m. The geometry is such that the body tapers towards the leading edge of the wing thus helping create vortices as explained earlier.

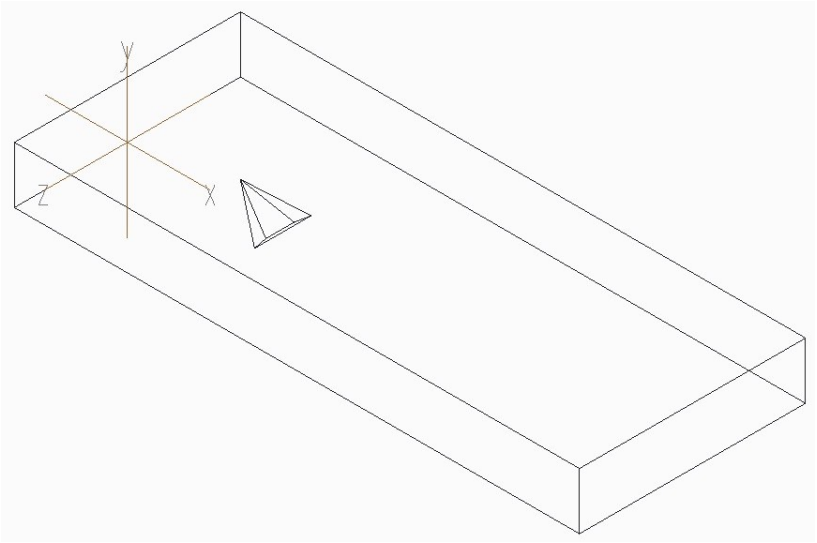

Figure 3-5 Isometric view of the trapezoidal delta wing with β =30˚

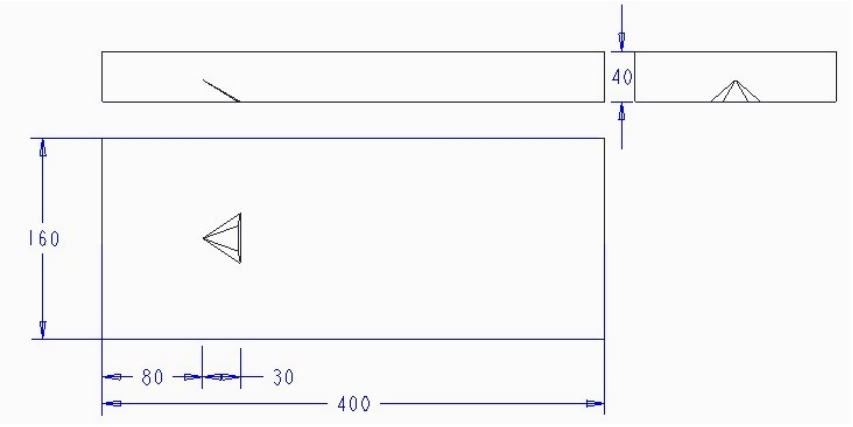

Figure 3-6 Orthographic view of a rectangular channel with trapezoidal delta wing at β = 30˚ (dimension in mm)

3.2.3 Delta Winglet Pair

The chord length of the delta winglet pair is 0.034641 m. The height is 0.02 m which is half of the channel. Different views of the delta winglet pair are shown in Figure 3-7 and Figure 3-8. The thickness of the DWP is $0.2*10^{-3}$ m and the winglet pairs are 0.01 m apart, transversely, from the leading edge. The attack angles taken in this study are 30˚ and 45˚ and the angle of incidence is kept as 30˚.

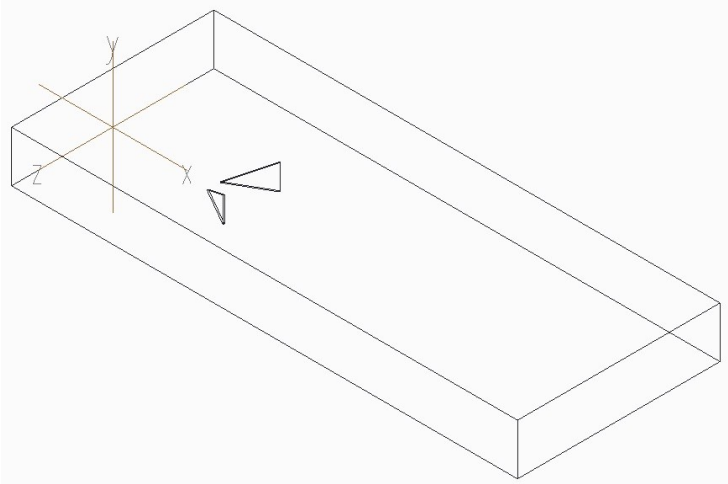

Figure 3-7 Isometric view of delta winglet pair at β = 30˚ (dimension in mm)

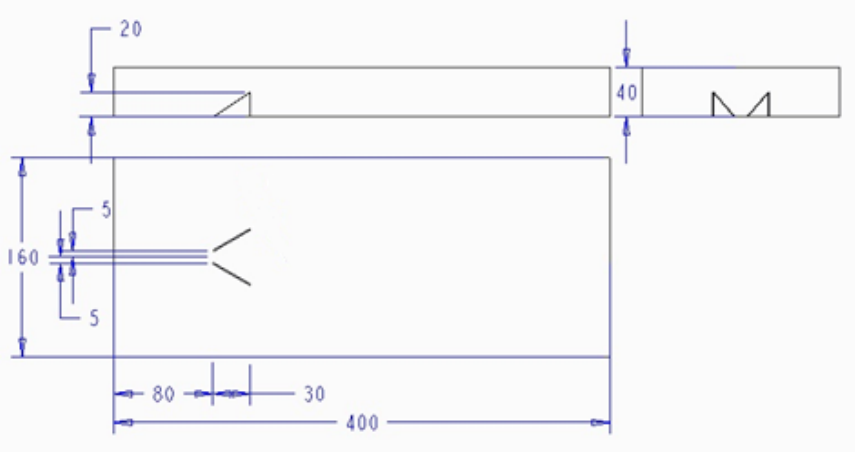

Figure 3-8 Orthographic view of delta winglet pair at β = 30˚ (dimension in mm)

3.3 Grid Generation

In this study ANSYS Workbench was used as a meshing tool. A local inflation control method was used to capture boundary layer formation at the lower wall of the channel. Shown in Figure 3-9 is meshed geometry where the first layer height has been given and five layers of inflation were given to help capture the boundary layer thus forming prisms or wedge elements. The remainder of the geometric model has maximum face size and maximum tetrahedral size proximity and curvature controlled meshed elements, forming a tetrahedral. The relevance center was set to medium to size the mesh away from the heated section.

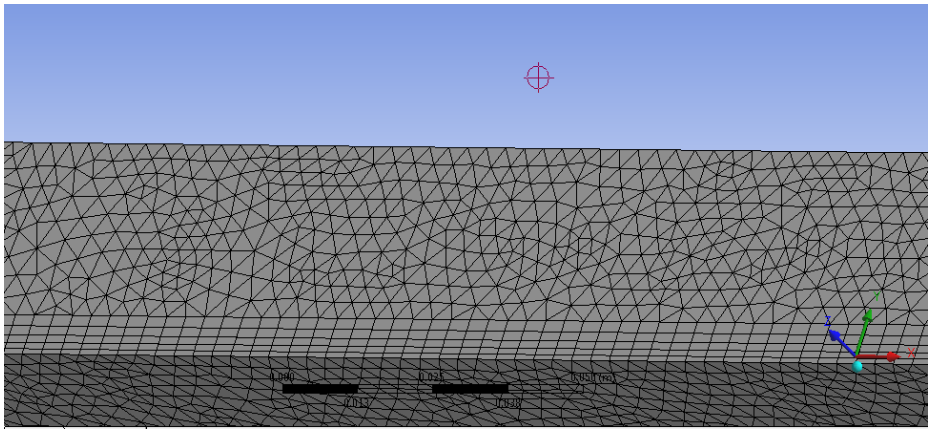

Figure 3-9 Mesh of the rectangular channel showing inflation layers

3.4 FLUENT Setup

FLUENT 12.0.16 was used for CFD analysis in this study. Importing the mesh files created in ANSYS Workbench, the model is setup to allow energy equation in a viscous laminar model. The fluid in this study is air with a constant density of 1.225 kg/m^3, dynamic viscosity of $1.7894*10^{-5}$ kg/m·s, the constant pressure specific heat is 1006.43 N/m·K, and thermal conductivity is 0.0242 W/m·K. The operating condition on the interior of the channel is fluid while the before mentioned boundary conditions are

applied on the rectangular channel including the inlet and outlet channel. A temperature of 400 K is applied on the surface of the heated section which is the bottom surface of the rectangular channel and all the surface of the vortex generator. The inlet has been given an inlet temperature of 300 K and a specific velocity based on the Reynolds number corresponding to the chosen Reynolds number. The outlet has zero pressure thus implying ambient condition. The walls of the whole channel, as well as surfaces of the vortex generator, have been given the no slip boundary condition. A second order upwind discretization method has been used for energy and momentum. Convergence is based on the absolute criteria of continuity, x velocity, y velocity and z velocity equal to 10^{-3} and energy equal to 10^{-6}. This means the solution will converge once the residuals reach the above mentioned mark. The model is computed from the inlet surface and 1000 iterations were given for the solution to converge.

3.5 Grid Independency Validation

Different sets of grids were considered for different geometries. The grid independence was conducted by simulating the channel with or without vortex generators at Re = 1000. The number of elements, ranging from 1.1 million to 2.1 million, were taken for different geometries and compared with the average surface Nusselt number and a maximum difference of 2% for $\overline{\mathrm{Nu}}$. This helped in deciding the element number for different geometry. The final element numbers for each of the geometries is shown in Table 3-1

Table 3-1 Showing element numbers for different geometries verifying grid independency validation

Geometry	**Element Numbers**
Rectangular channel without VG	1185668
Delta Wing with β=30˚	1514004
Delta Wing with β=45˚	1518326
Trapezoidal Delta Wing with β=30˚	1357503
Trapezoidal Delta Wing with β=45˚	1354832
Delta Winglet Pair with β=30˚	1843333
Delta Winglet Pair with β=45˚	2100991

Chapter 4

Results and Discussions

This study on heat transfer enhancement characteristics for a rectangular channel for a laminar flow conditions on different vortex generators gives a better idea of the use of specific vortex generator on the basis of average surface Nusselt number ratio, Friction factor ratio, and performance evaluation parameter.

4.1 Delta Wing

The downwash flow towards the wall is observed between vortices while the upwash flow is observed in the outer region of the vortices as shown in Figure 4-1.

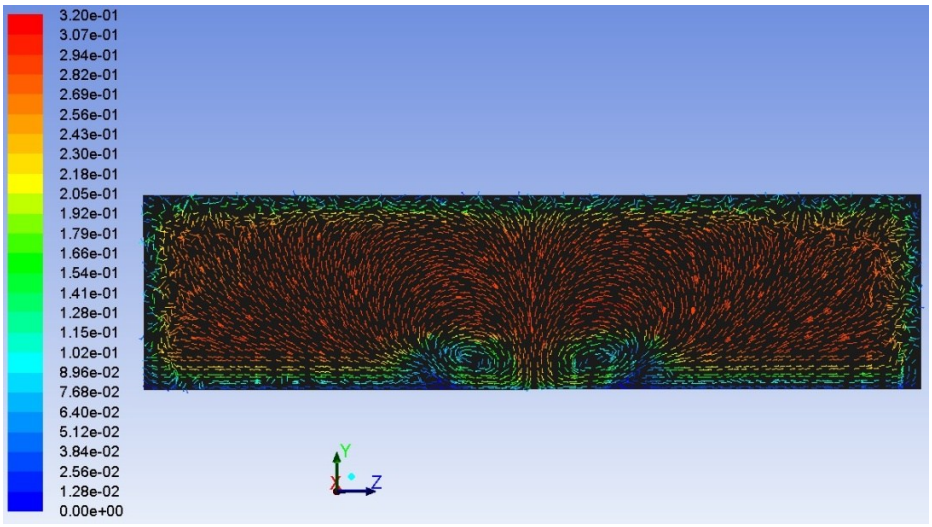

Figure 4-1 Velocity vectors of velocity (m/s) showing the vortices generated in a delta wing at Re = 1000, x = 0.52 m, and β = 30˚

As seen in Figure 4-2, the vortices generated are not strong enough to last the entire length of the channel and thus lose strength soon enough which is not good for heat transfer enhancement. Heat transfer requires the vortex generators to generate vortices along the downstream of the vortex generator.

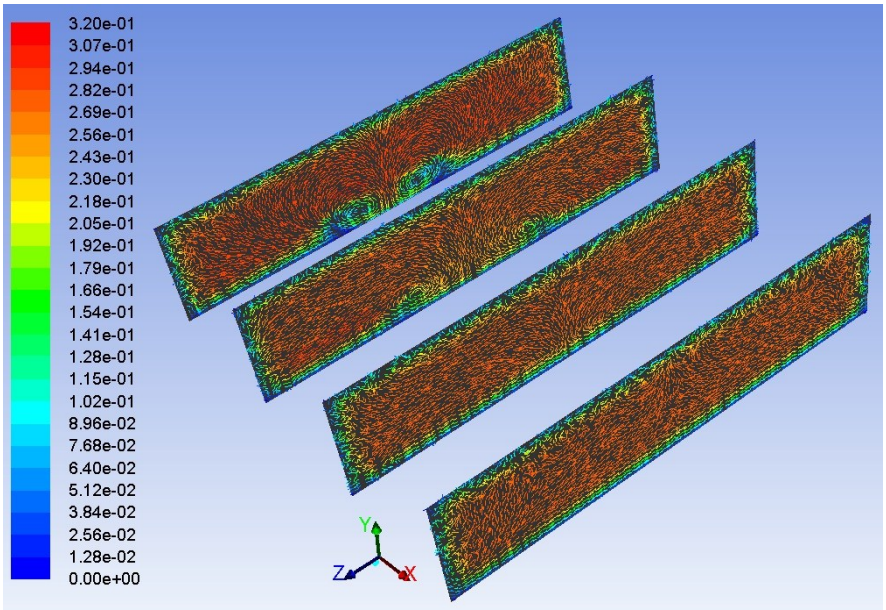

Figure 4-2 Velocity vectors of velocity (m/s) showing the vortices generated in a delta wing at x = 0.52 m, 0.57 m, 0.62 m, and 0.67 m at Re = 1000 and β = 30˚

Since the vortices generated are not strong for a delta wing, the boundary layer only thickens very close downstream to the vortex generator. Thus the boundary layer quickly thickens downstream of the flow. Figure 4-3 and Figure 4-4 shows, the vectors and contours of the static temperature and the thinning of the boundary layer only close to the vortex generator downstream.

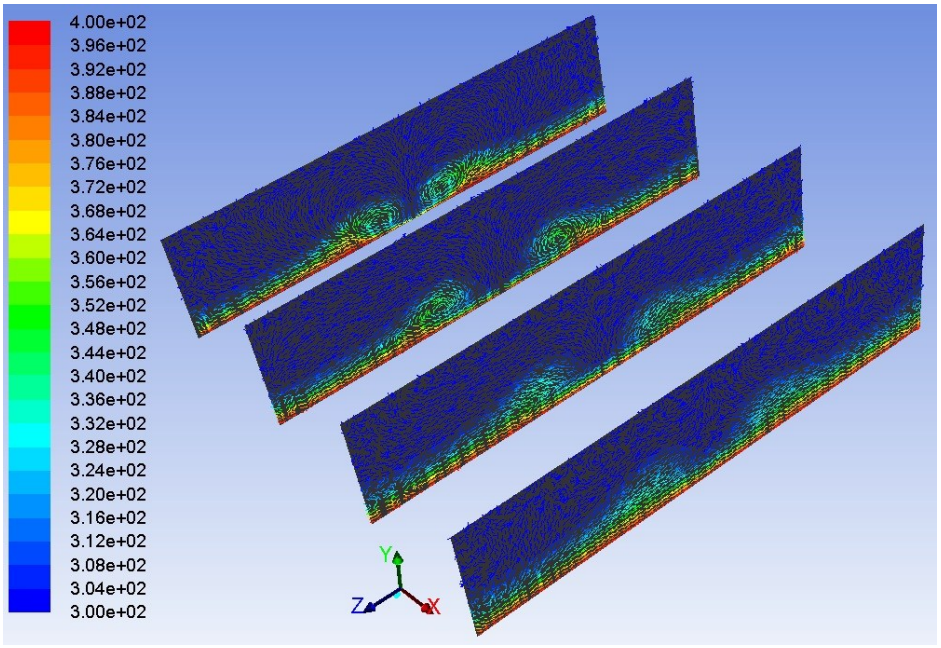

Figure 4-3 Velocity vectors of Static Temperature (K) showing the vortices generated in a delta wing at x = 0.52 m, 0.57 m, 0.62 m, and 0.67 m at Re = 1000 and β = 30˚

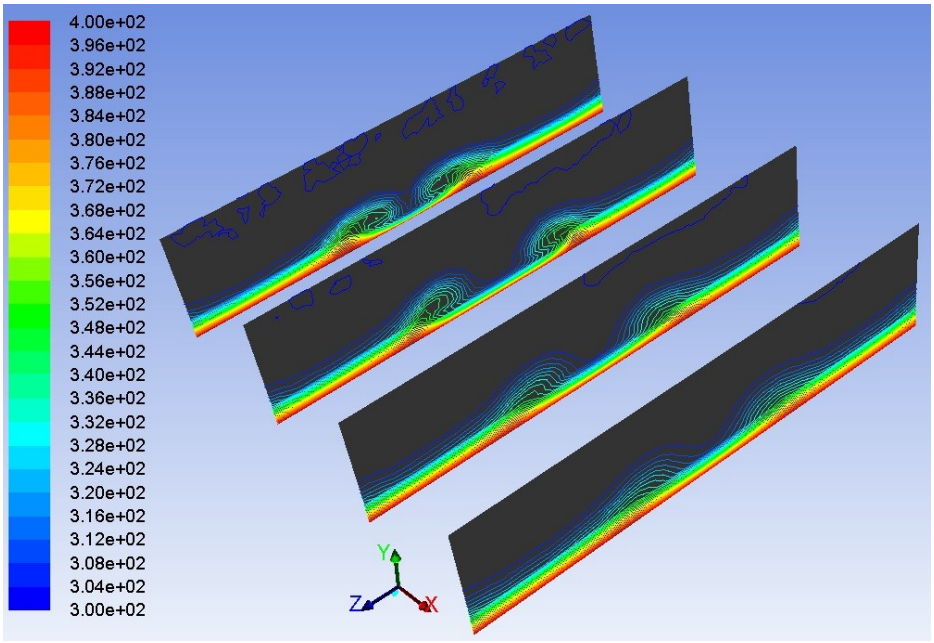

Figure 4-4 Contours of Static Temperature (K) showing the vortices generated in a delta wing at x = 0.52 m, 0.57 m, 0.62 m, and 0.67 m at Re = 1000 and β = 30˚

As shown in Figure 4-5, the average surface Nusselt number ratio increases with the increase in Reynolds number and the ratio is always greater than one, signifying the heat transfer enhancement is taking place.

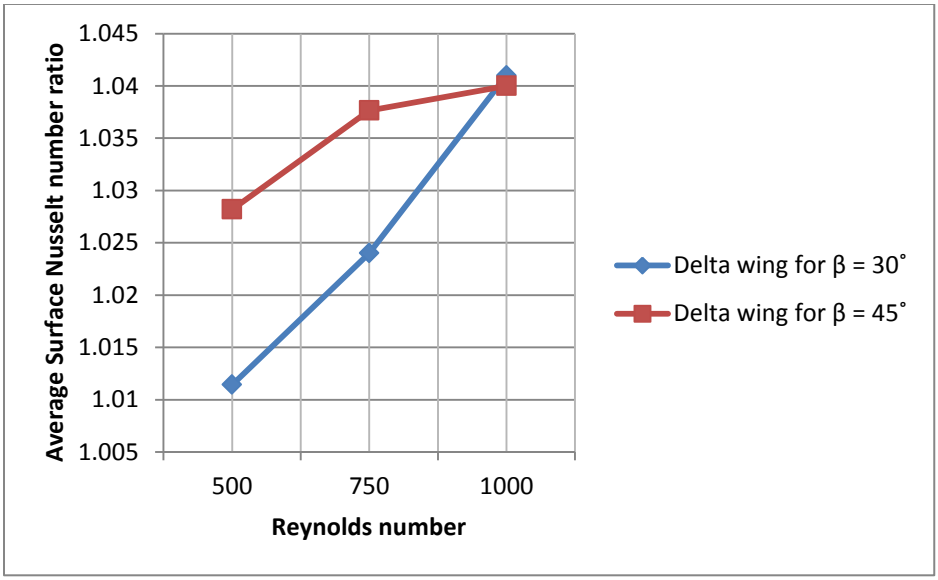

Figure 4-5 Comparison of average surface Nusselt number ratio with Reynolds number for delta wing at angle of attack of 30° and 45°

The friction factor is also always greater than one for any protruding device since it means that there is pressure loss due to form drag and skin friction drag which are both evident in this case because of the geometry. Shown in Figure 4-6 is the ratio of Friction factor with that of Reynolds number which shows with the increase in friction factor ratio; the Reynolds number also increases. The prominent and consistent increase in the Friction factor means that the body generates a great deal of drag and, hence, the friction factor for β = 45˚ is more than that of β = 30˚. Also, shown in Figure 4-7 is the Performance Evaluation Parameter which decreases as the Reynolds number increases.

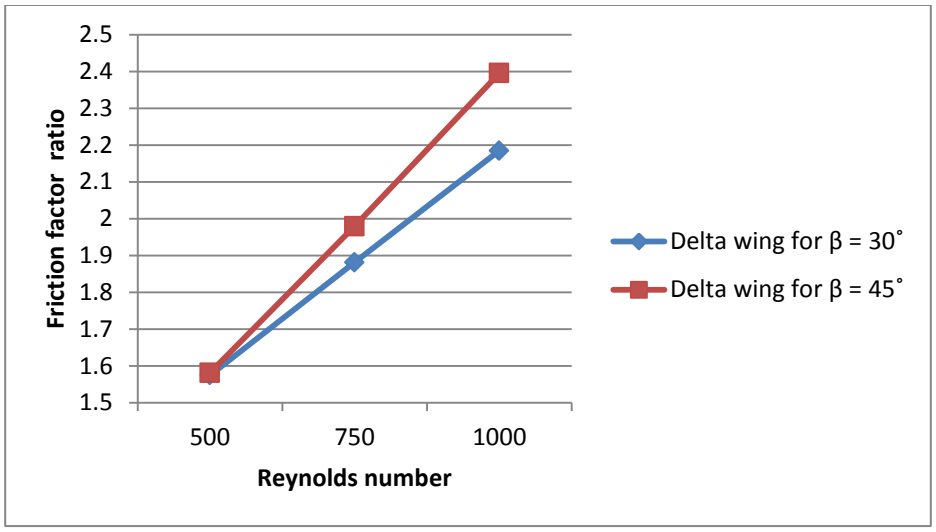

Figure 4-6 Comparison of Friction factor ratio with Reynolds number for delta wing at angle of attack of 30° and 45°

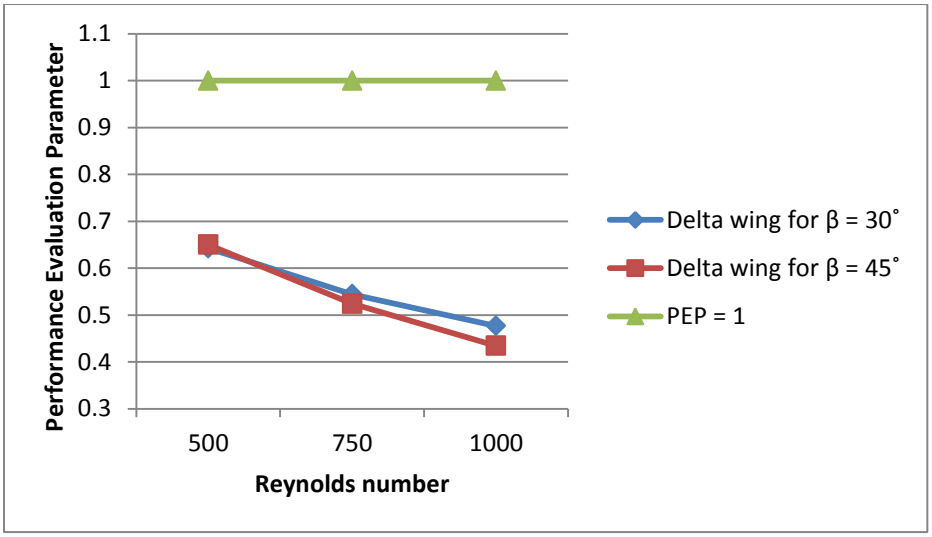

Figure 4-7 Comparison of Performance Evaluation Parameter with Reynolds number for delta wing at angle of attack of 30° and 45°

4.2 Trapezoidal Delta Wing

In a trapezoidal delta wing, the downwash is also observed towards the wall between two vortices generated while the upwash is on the outer region of the vortices as shown in Figure 4-8.

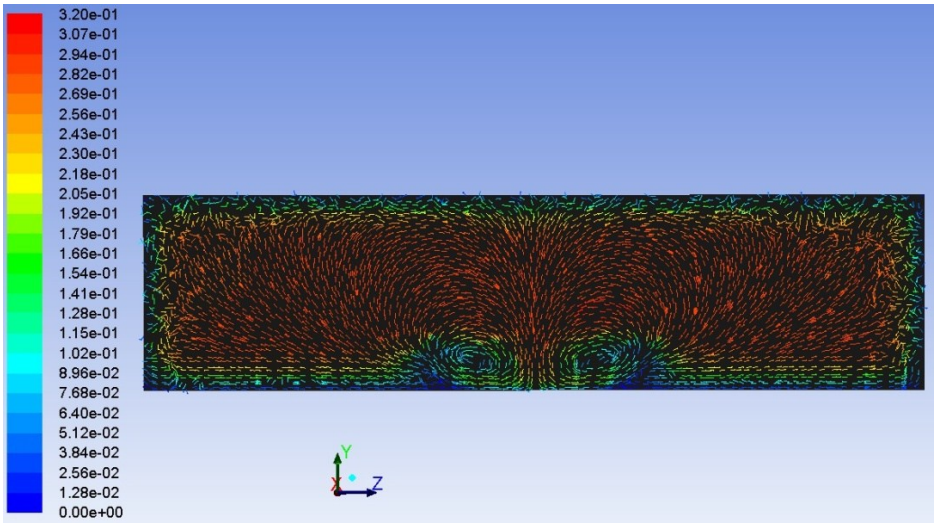

Figure 4-8 Velocity vectors of velocity (m/s) showing the vortices generated in a trapezoidal delta wing at Re = 1000, x = 0.52 m, and β = 30˚

The vortices generated are visible in the downstream and help in heat transfer enhancement while the strength of the vortices grow weaker along the downstream almost as quickly as a delta wing as shown in Figure 4-9. The thinning of the boundary layer takes place nearer to the wing downstream. Thus, the boundary layer thickens further downstream similar to that of a delta wing.

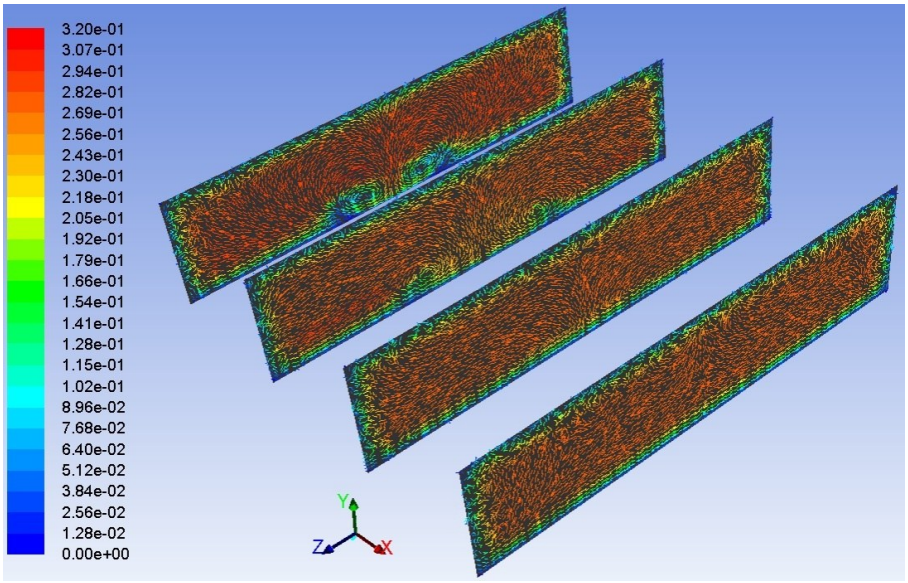

Figure 4-9 Velocity vectors of velocity (m/s) showing the vortices generated in a trapezoidal delta wing at x = 0.52 m, 0.57 m, 0.62 m, and 0.67 m at Re = 1000 and β = 30˚

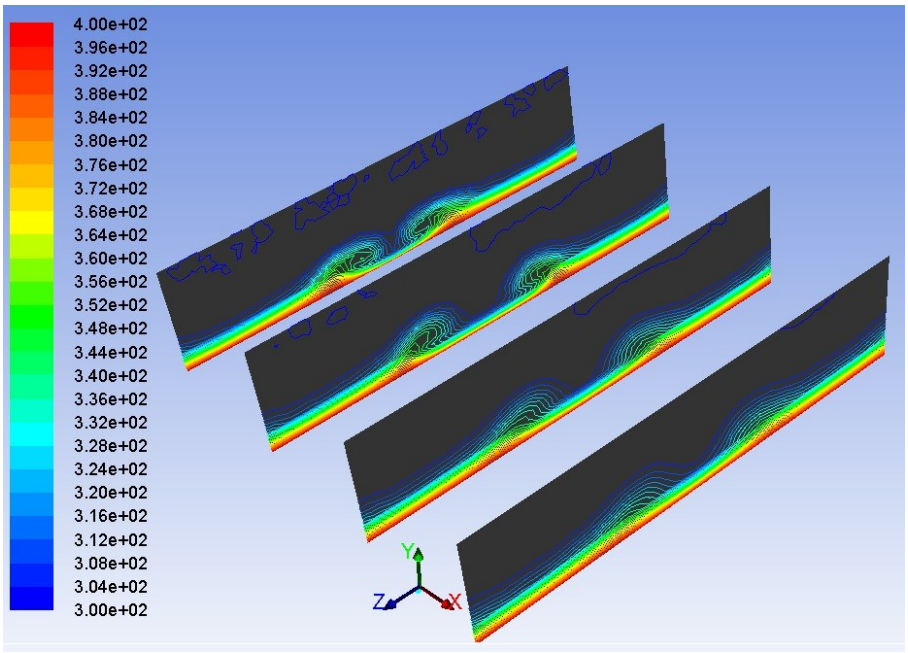

Figure 4-10 Contours of Static Temperature (K) showing the vortices generated in a trapezoidal delta wing at x = 0.52 m, 0.57 m, 0.62 m, and 0.67 m at Re = 1000 and β = 30˚

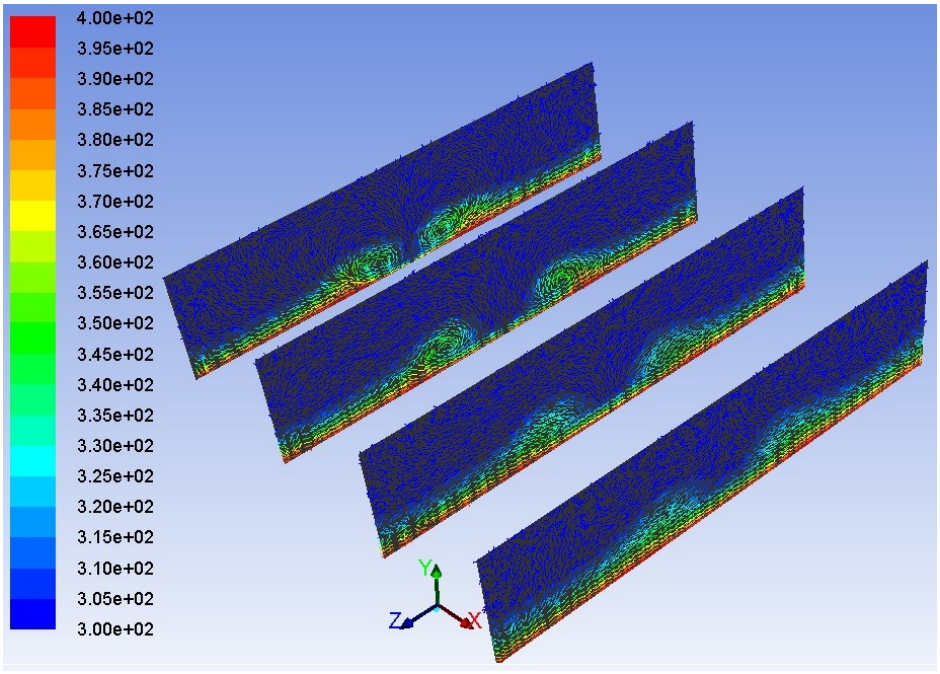

Figure 4-11 Velocity vectors of Static Temperature (K) showing the vortices generated in a trapezoidal delta wing at x = 0.52 m, 0.57 m, 0.62 m, and 0.67 m at Re = 1000 and β = 30˚

As shown in Figure 4-12, the average surface Nusselt number ratio increases with an increase in Reynolds number and so does the Friction factor ratio as shown in Figure 4-13. But, as mentioned earlier, the friction factor ratio depends on the attack angle and that is the reason the friction factor is higher for greater values of attack angle, β. The performance evaluation factor is shown to be higher for lower Reynolds number since the convective heat transfer is greater while the frictional losses, or pressure losses, are minimal. But as compared to the delta wing, even though the average surface Nusselt number ratio is prominently higher, the distinguished pressure loss does not lead to a notable change in the performance evaluation parameter.

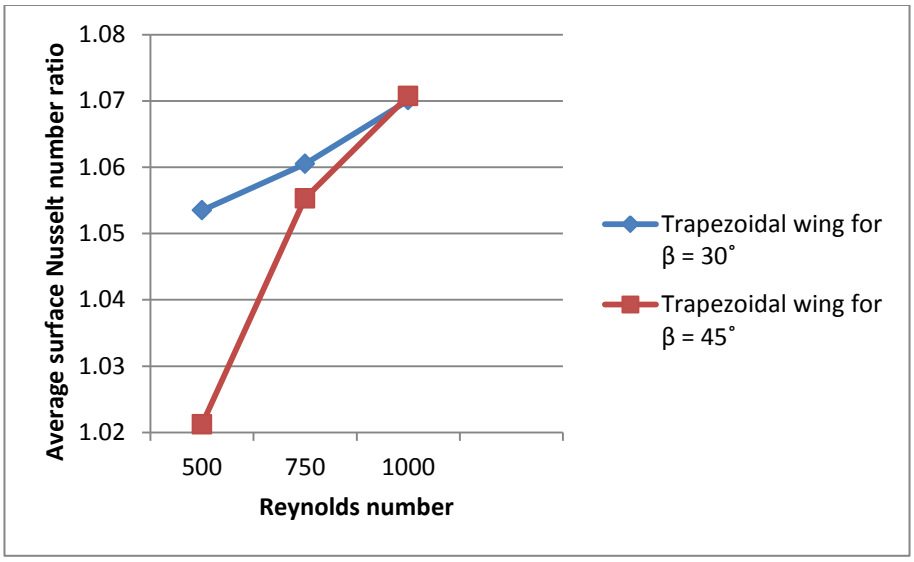

Figure 4-12 Comparison of average surface Nusselt number ratio with Reynolds number for trapezoidal delta wing at angle of attack of 30° and 45°

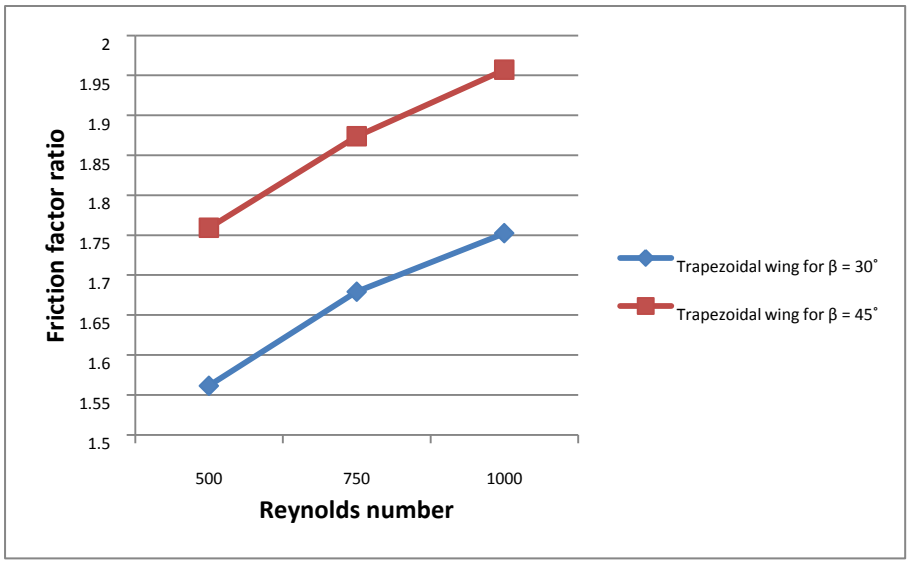

Figure 4-13 Comparison of Friction factor ratio with Reynolds number for trapezoidal delta wing at angle of attack of 30° and 45°

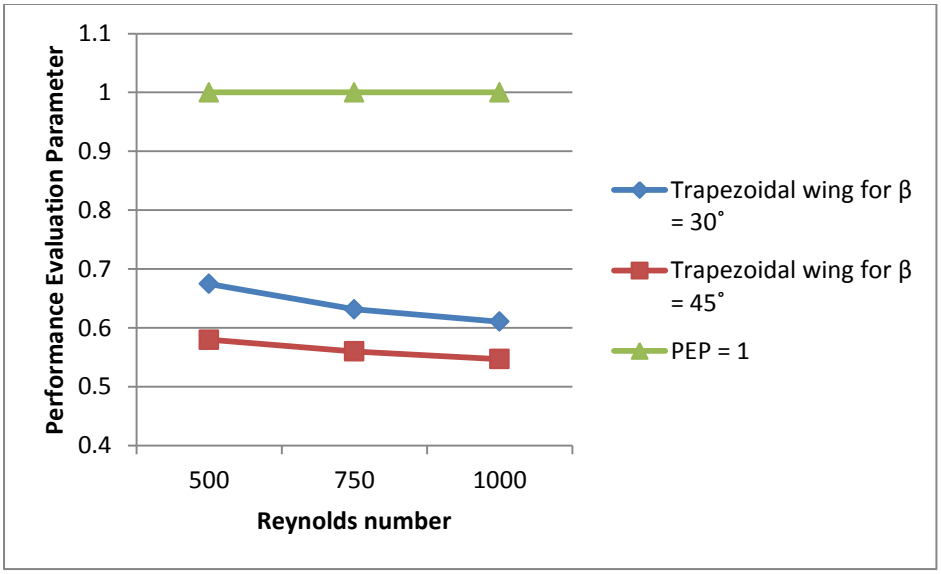

Figure 4-14 Comparison of Performance Evaluation Factor with Reynolds number for trapezoidal delta wing at angle of attack of 30° and 45°

4.3 Delta Winglet Pair

The downwash flow towards the wall is observed between vortices while the upwash flow is observed away from the wall on the outside region of the vortices generated as shown in Figure 4-15. As the vortices develop along the downstream of the vortex generators, the magnitude of their velocity vectors reduces and the interval between them decreases as seen in Figure 4-16.

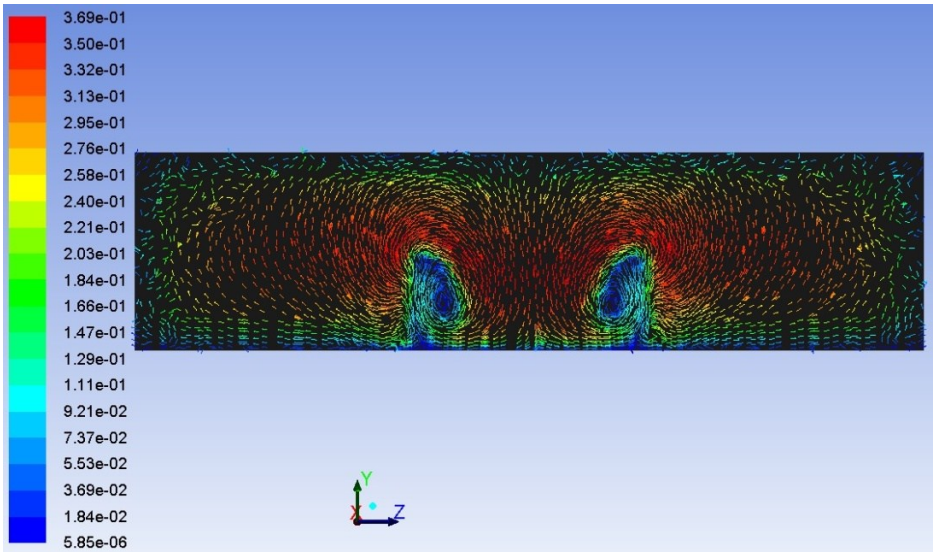

Figure 4-15 Velocity vectors of velocity (m/s) showing the vortices generated in a delta winglet pair at Re = 1000, x = 0.52 m, and β = 30˚

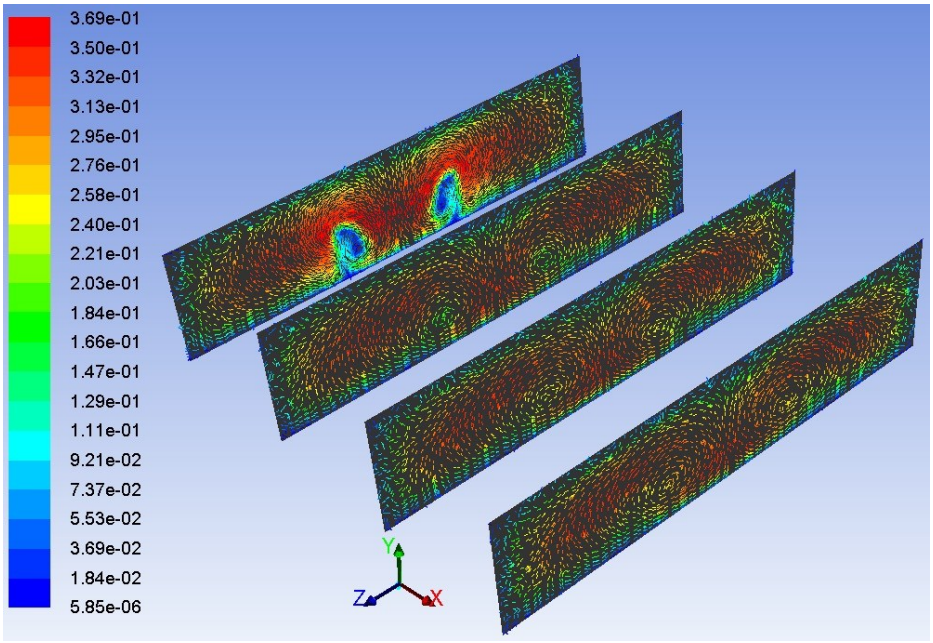

Figure 4-16 Velocity vectors of velocity (m/s) downstream of the wing at x = 0.52 m, 0.57 m, 0.62 m, and 0.67 m in a delta winglet pair at Re = 1000 and β = 30˚

It can be seen that the interaction of the vortices affects the change of boundary layer thickness. Thinning of the boundary layer between the vortices is observed, while the boundary layer is thickened on the upwash region. As the secondary velocities decrease in magnitude in the downwash region, the boundary layer grows. It is also noted that the vortices do not interact with each other downstream but substantial interaction between the vortices and the boundary layer is noticed. Similar to the contours of velocity, the temperature contours are thickened in the upwash region and thinned in the downwash region. In Figure 4-17 and Figure 4-18, the distortion or thinning of the thermal boundary layer is not prominent since it is at an early stage of development. It builds up further downstream.

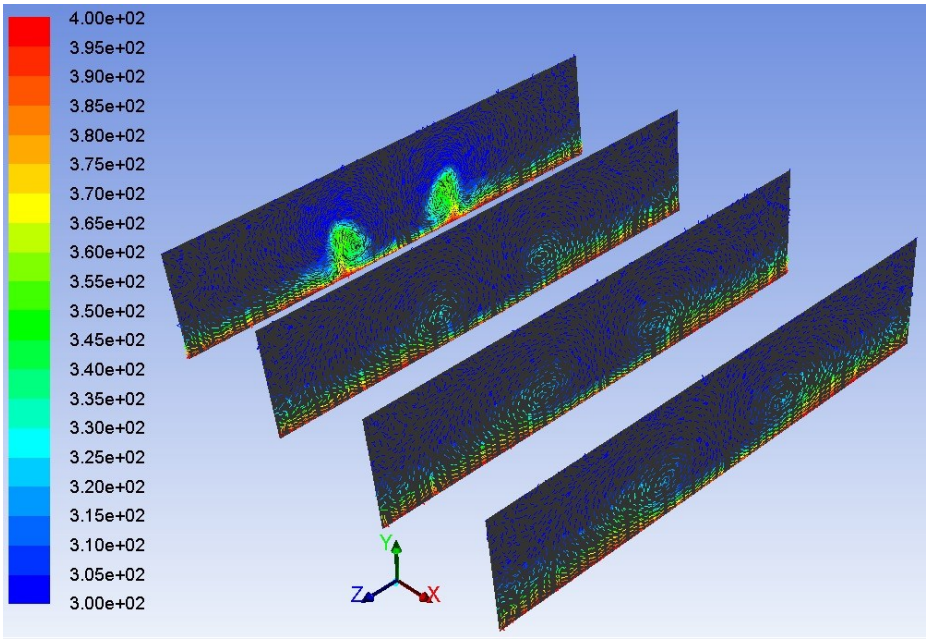

Figure 4-17 Velocity vectors of Static Temperature (K) downstream of the wing at x = 0.52 m, 0.57 m, 0.62 m, and 0.67 m in a delta winglet pair at Re = 1000 and β = 30˚

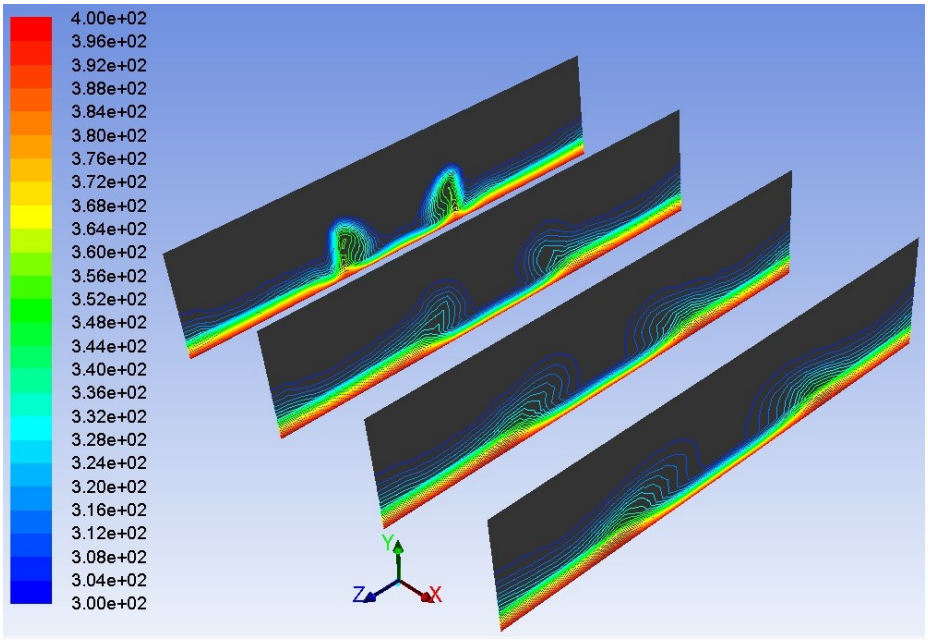

Figure 4-18 Contours of Static Temperature (K) downstream of the wing at x = 0.52 m, 0.57 m, 0.62 m, and 0.67 m in a delta winglet pair at Re = 1000 and β = 30˚

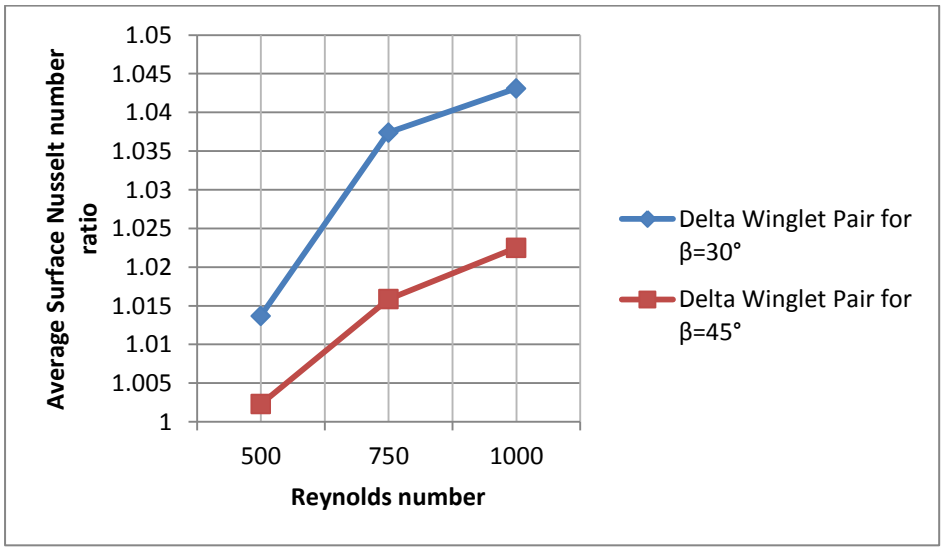

Figure 4-19 Comparison of average surface Nusselt number ratio with Reynolds number for delta winglet pair at angle of attack of 30° and 45°

As shown in Figure 4-19, it is observed that the ratio of the average surface Nusselt number of the channel is greater than one which means the heat transfer enhancement takes place in the channel with vortex generator much more than in a channel without any vortex generator. Also, the average surface Nusselt number ratio increases with the increase in Reynolds number. In Figure 4-20, the ratio of the friction factor of the channel is shown with and without the vortex generator (f / f_0) and is observed to be greater than one which means that the vortex generator produces form drag and skin friction drag leading to a higher difference in pressure loss

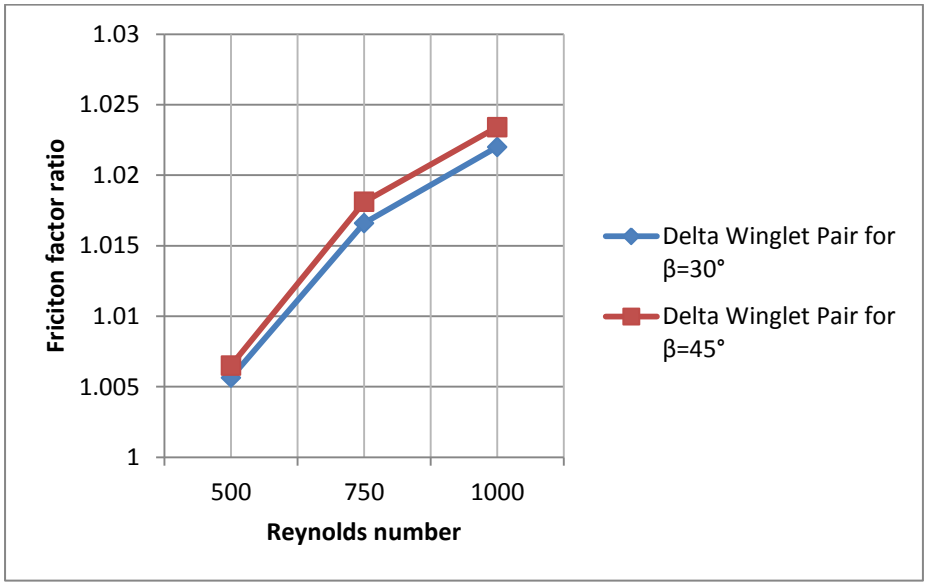

Figure 4-20 Comparison of Friction factor ratio with Reynolds number for delta winglet pair at angle of attack of 30° and 45°

In Figure 4-21, the performance evaluation parameter $((Nu / Nu_0) / (f / f_0))$ is shown concluding that the performance of the winglet is better at an attack angle of 30° rather than an attack angle of 45°.

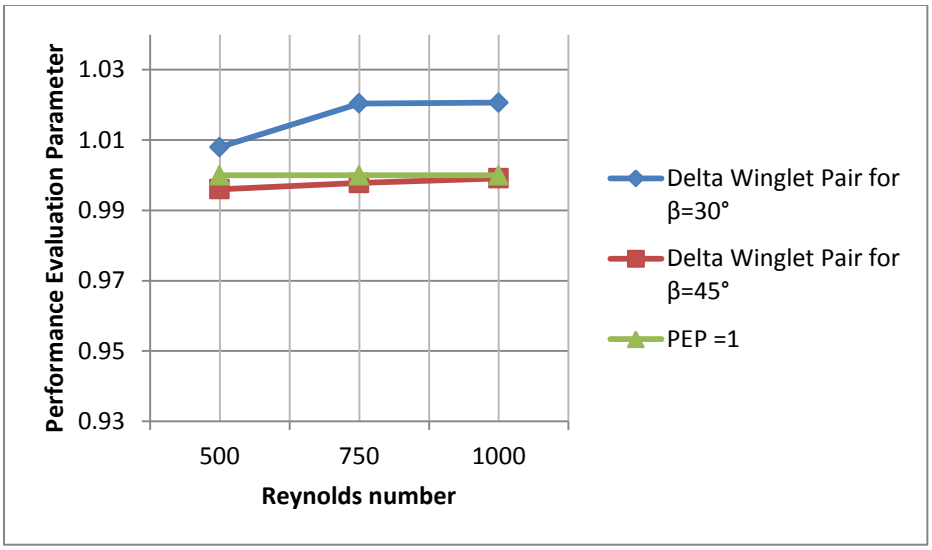

Figure 4-21 Comparison of Performance Evaluation Parameter with Reynolds number for delta winglet pair at angle of attack of 30° and 45°

Chapter 5

Conclusion

In this study, different longitudinal vortex generators such as the delta wing, trapezoidal delta wing and delta winglet pair were numerically studied and compared on the basis of average surface Nusselt number ratio, Friction factor ratio, and Performance Evaluation Parameter to understand the advantages and disadvantages of each using FLUENT. The following was concluded after this study.

- The average surface Nusselt number ratio for a delta wing at attack angles of 30˚ and 45˚ shows that the heat transfer enhancement takes place to some extent and a higher attack angle produces higher heat augmentation but at the cost of pressure loss. It is also seen that the pressure loss is greater at higher attack angles. Thus the overall performance evaluation parameter goes below one. Hence, the delta wings are seldom used in heat exchangers. The main use of delta wings is in cases where one needs high average surface Nusselt number ratio and pressure loss is no concern. The low production, operating and manufacturing cost also add to the advantages of using delta wings.
- The average surface Nusselt number ratio for a trapezoidal delta wing is much higher than that of delta wing at the same attack angles and same chord length of the wing. The only advantage is that the trapezoidal wing has a sharp leading edge which helps in the early generation of primary vortices and, thus, has higher average surface Nusselt number than the delta wing. The friction factor in this case too depends on the attack angle and, hence, higher attack angles produce higher pressure losses. It is seen that the performance evaluation parameter in trapezoidal wing is less than one but

greater than that of delta wing. Despite this, the trapezoidal wing is not preferred over delta wing because of its unusual structure and cost of manufacturing.

- The average surface Nusselt number ratio for a delta winglet pair is as high as that of a trapezoidal wing keeping the same chord length but the friction factor is very low and close to one, which is lower than the other two geometries. The Friction factor ratio is greater for higher attack angles. But, the performance evaluation factor is greater for the attack angle = 30˚ than that of β = 45˚. It is seen that the performance evaluation parameter is higher than one when Re > 500 for β = 30˚ while for β = 45˚ the Re should be around 1000. The delta winglet pairs are preferred over other geometries for obvious reasons and in case pressure loss is a concern.
- Not only do the plots conclude the above mentioned point but the same conclusion can be made from the figures in chapter 4. The vortices generated in a delta winglet pair create more disturbances in the flow than in the delta wing or trapezoidal wing.
- Boundary layer thinning occurs in all the geometries but is prominent and of higher order in a delta winglet pair and is visible downstream of the flow.
- Drag is formed in all geometries that are protruding when air flows through the channel but it is less in the case of a delta winglet pair. It is comparatively higher is the cases of delta wing and trapezoidal wing. Also, greater angles of attack produce greater form drag and, thus, higher values of friction.

Chapter 6

Future Recommendations

Based on this study, a great deal of work can be done for heat transfer enhancement using vortex generator in the future. Here are a few ways to improve the performance enhancement factor or average surface Nusselt number ratio:

- Improve the geometry by using thinner width delta winglet pair. It has been seen that thinner plates reduce the friction factor ratio while negligibly changing the average surface Nusselt number ratio and, hence, increasing the Performance Evaluation Parameter.
- It may prove to be useful to try heat exchange enhancement by using delta winglet pair over higher ranges of Reynolds number.
- It may prove to be useful to change the geometry and try out a new geometry all together. Blending the triangular faces of a delta winglet pairs to spiral in or against the direction of the vortex could be useful.

Appendix A

Nomenclature

a	=	transverse distance between the winglet pair (m)
A	=	heat transfer surface area (m^2)
A_1	=	primary attachment line
A_2	=	secondary attachment line
B	=	width of the channel (m)
b	=	thickness of the vortex generator (m)
CFD	=	common flow down configuration for a delta winglet pair or Computational Fluid Dynamics where specified
CFU	=	common flow up configuration for a delta winglet pair
C_p	=	specific heat capacity of the fluid at constant pressure (J / (kg·K))
DWP	=	delta winglet pair vortex generator
f	=	Darcy's Friction factor (dimensionless)
f_0	=	Darcy's Friction factor ratio for a rectangular channel without vortex generator (dimensionless)
f / f0	=	Friction factor ratio (dimensionless)
h	=	height of the vortex generator (m) or average heat transfer coefficient (W/m^2K)
H	=	height of the channel (m)
H_d	=	hydraulic diameter or characteristic length (m)
K	=	Thermal Conductivity (W/m·K)
l	=	chord length of the vortex generator (m)
L	=	length of the channel (m)
LVG	=	longitudinal vortex generators
Nu	=	Nusselt number (dimensionless)
$\overline{Nu}$	=	average surface Nusselt number (dimensionless)
Nu_0	=	Nusselt number for a rectangular channel without a vortex generator

$\overline{Nu_0}$	=	average surface Nusselt number for a rectangular channel without a vortex generator (dimensionless)
$\frac{\overline{Nu}}{\overline{Nu_0}}$	=	non-dimensional average surface Nusselt number ratio (dimensionless)
p	=	static pressure (Pa)
P^*	=	non-dimensional static pressure (dimensionless)
PEP	=	performance evaluation parameter $((Nu/Nu_0) / (f/f_0))$
Pr	=	Prandtl number (dimensionless)
Q	=	heat transfer capacity of the fluid (W)
Re	=	Reynolds number (dimensionless)
RWP	=	rectangular winglet pair vortex generators
s	=	stream wise distance from the heated rectangular channel to the leading of the vortex generator (m)
S_1	=	primary separation line
S_2	=	secondary separation line
T	=	temperature (K)
T^*	=	non-dimensional temperature (dimensionless)
T_{in}	=	temperature at inlet (K)
T_{out}	=	temperature at outlet (K)
T_w	=	temperature at wall (K)
V	=	mean velocity of fluid flow (m/s)
u	=	velocity in X direction (m/s)
u^*	=	non-dimensional velocity in X-direction (dimensionless)
v	=	velocity in Y direction (m/s)
v^*	=	non-dimensional velocity in Y-direction (dimensionless)
w	=	velocity in Z direction (m/s)

w^*	=	non-dimensional velocity in Z-direction (dimensionless)
x	=	distance in X direction (m)
x^*	=	non-dimensional distance in X-direction (dimensionless)
y	=	distance in Y direction (m)
y^*	=	non-dimensional distance in Y-direction (dimensionless)
z	=	distance in Z direction (m)
z^*	=	non-dimensional distance in Z-direction (dimensionless)
α	=	angle of incidence used in delta winglet pair (degrees) or thermal diffusivity of the fluid where mentioned (m^2/s)
β	=	angle of attack of longitudinal vortex generators (degrees)
ΔT	=	temperature difference (K)
ϑ	=	kinematic viscosity of the fluid (m^2/s)
μ	=	dynamic viscosity of the fluid (kg / (m·s))
ρ	=	density of the fluid (kg/m^3)

References

[1] Anderson, J.D., 2001, "Fundamentals of aerodynamics," McGraw-Hill New York.

[2] Biswas, G., Torii, K., Fujii, D., 1996, "Numerical and Experimental Determination of Flow Structure and Heat Transfer Effects of Longitudinal Vortices in a Channel Flow," International Journal of Heat and Mass Transfer, **39**(16) pp. 3441-3451.

[3] Chen, Y., Fiebig, M., and Mitra, N. K., 2000, "Heat Transfer Enhancement of Finned Oval Tubes with Staggered Punched Longitudinal Vortex Generators," International Journal of Heat and Mass Transfer, **43**(3) pp. 417-435.

[4] Compton, D. A., and Johnston, J. P., 2012, "Streamwise Vortex Production by Pitched and Skewed Jets in a Turbulent Boundary Layer," AIAA Journal, **30**(3).

[5] Deb, P., Biswas, G., and Mitra, N., 1995, "Heat Transfer and Flow Structure in Laminar and Turbulent Flows in a Rectangular Channel with Longitudinal Vortices," International Journal of Heat and Mass Transfer, **38**(13) pp. 2427-2444.

[6] Ferrouillat, S., Tochon, P., Garnier, C., 2006, "Intensification of Heat-Transfer and Mixing in Multifunctional Heat Exchangers by Artificially Generated Streamwise Vorticity," Applied Thermal Engineering, **26**(16) pp. 1820-1829.

[7] Fiebig, M., 1998, "Vortices, Generators and Heat Transfer," Chemical Engineering Research and Design, **76**(2) pp. 108-123.

[8] Fiebig, M., 1995, "Embedded Vortices in Internal Flow: Heat Transfer and Pressure Loss Enhancement," International Journal of Heat and Fluid Flow, **16**(5) pp. 376-388.

[9] Gentry, M., and Jacobi, A., 2002, "Heat Transfer Enhancement by Delta-Wing-Generated Tip Vortices in Flat-Plate and Developing Channel Flows," Journal of Heat Transfer, **124**(6) pp. 1158-1168.

[10] Gentry, M., and Jacobi, A., 1997, "Heat Transfer Enhancement by Delta-Wing Vortex Generators on a Flat Plate: Vortex Interactions with the Boundary Layer," Experimental Thermal and Fluid Science, **14**(3) pp. 231-242.

[11] Hiravennavar, S., Tulapurkara, E., and Biswas, G., 2007, "A Note on the Flow and Heat Transfer Enhancement in a Channel with Built-in Winglet Pair," International Journal of Heat and Fluid Flow, **28**(2) pp. 299-305.

[12] Jacobi, A., and Shah, R., 1995, "Heat Transfer Surface Enhancement through the use of Longitudinal Vortices: A Review of Recent Progress," Experimental Thermal and Fluid Science, **11**(3) pp. 295-309.

[13] Johnston, J. P., and Nishi, M., 2012, "Vortex Generator Jets-Means for Flow Separation Control," AIAA Journal, **28**(6).

[14] Kakaç, S., Bergles, A.E., Mayinger, F., 1999, "Heat transfer enhancement of heat exchangers," Springer,.

[15] Kim, W., and Patel, V., 1994, "Influence of Streamwise Curvature on Longitudinal Vortices Imbedded in Turbulent Boundary Layers," Computers & Fluids, **23**(5) pp. 647-673.

[16] Li, J., Wang, S., Chen, J., 2011, "Numerical Study on a Slit Fin-and-Tube Heat Exchanger with Longitudinal Vortex Generators," International Journal of Heat and Mass Transfer, **54**(9) pp. 1743-1751.

[17] Mahmood, G., Hill, M., Nelson, D., 2001, "Local Heat Transfer and Flow Structure on and Above a Dimpled Surface in a Channel," Journal of Turbomachinery, **123**(1) pp. 115-123.

[18] Mahmood, G., and Ligrani, P., 2002, "Heat Transfer in a Dimpled Channel: Combined Influences of Aspect Ratio, Temperature Ratio, Reynolds Number, and Flow Structure," International Journal of Heat and Mass Transfer, **45**(10) pp. 2011-2020.

[19] Ohadi, M., Dessiatoun, S., Singh, A., 1994, "EHD Enhancement of boiling/condensation Heat Transfer of Alternate Refrigerants," Progress Report no.EHDC Prog.Rep, **5**.

[20] Ohadi, M., Sharaf, N., and Nelson, D., 1991, "Electrohydrodynamic Enhancement of Heat Transfer in a Shell-and Tube Heat Exchanger," EXPERIMENTAL HEAT TRANSFER an International Journal, **4**(1) pp. 19-39.

[21] Ortmanns, J., and Kähler, C. J., 2007, "The Effect of a Single Vortex Generator Jet on the Characteristics of a Turbulent Boundary Layer," International Journal of Heat and Fluid Flow, **28**(6) pp. 1302-1311.

[22] Schubauer, G. B., and Spangenberg, W., 1960, "Forced Mixing in Boundary Layers," Journal of Fluid Mechanics, **8**(01) pp. 10-32.

[23] Sohankar, A., 2007, "Heat Transfer Augmentation in a Rectangular Channel with a Vee-Shaped Vortex Generator," International Journal of Heat and Fluid Flow, **28**(2) pp. 306-317.

[24] Tian, L., He, Y., Lei, Y., 2009, "Numerical Study of Fluid Flow and Heat Transfer in a Flat-Plate Channel with Longitudinal Vortex Generators by Applying Field Synergy Principle Analysis," International Communications in Heat and Mass Transfer, **36**(2) pp. 111-120.

[25] Tiggelbeck, S., Mitra, N., and Fiebig, M., 1992, "Flow Structure and Heat Transfer in a Channel with Multiple Longitudinal Vortex Generators," Experimental Thermal and Fluid Science, **5**(4) pp. 425-436.

[26] Torii, K., Kwak, K., and Nishino, K., 2002, "Heat Transfer Enhancement Accompanying Pressure-Loss Reduction with Winglet-Type Vortex Generators for Fin-Tube Heat Exchangers," International Journal of Heat and Mass Transfer, **45**(18) pp. 3795-3801.

[27] Wang, Q., Chen, Q., Wang, L., 2007, "Experimental Study of Heat Transfer Enhancement in Narrow Rectangular Channel with Longitudinal Vortex Generators," Nuclear Engineering and Design, **237**(7) pp. 686-693.

[28] Webb, R. L., and Kim, N. H., 1994, "Principles of Enhanced Heat Transfer,".

[29] Wu, J. M., and Tao, W. Q., 2008, "Numerical Study on Laminar Convection Heat Transfer in a Channel with Longitudinal Vortex Generator. Part B: Parametric Study of Major Influence Factors," International Journal of Heat and Mass Transfer, **51**(13–14) pp. 3683-3692.

[30] Wu, J. M., and Tao, W. Q., 2008, "Numerical Study on Laminar Convection Heat Transfer in a Rectangular Channel with Longitudinal Vortex Generator. Part A: Verification of Field Synergy Principle," International Journal of Heat and Mass Transfer, **51**(5–6) pp. 1179-1191.

[31] Yang, J., Seo, J., and Lee, K., 2001, "A Numerical Analysis on Flow Field and Heat Transfer by Interaction between a Pair of Vortices in Rectangular Channel Flow," Current Applied Physics, **1**(4) pp. 393-405.

[32] Zhang, X., and Collins, M. W., 1993, "Flow and Heat Transfer in a Turbulent Boundary Layer through Skewed and Pitched Jets," AIAA Journal, **31**(9) pp. 1590-1599.

[33] Zhu, J., Fiebig, M., and Mitra, N., 1995, "Numerical Investigation of Turbulent Flows and Heat Transfer in a Rib-Roughened Channel with Longitudinal Vortex Generators," International Journal of Heat and Mass Transfer, **38**(3) pp. 495-501.

[34] Zohir, A., "The Influence of Pulsation on Heat Transfer in a Heat Exchanger for Parallel and Counter Water Flows,"

Biographical Information

Ninad Maniar comes from a humble family in India. His father is a financial advisor and his mother is a homemaker. His brother influenced him in many stages of his life and he is the primary reason for his interest in Mechanical Engineering. To fulfill his interest and pursue Masters he enrolled in The University of Texas at Arlington. On completion of his Masters, he plans to pursue his career as a Mechanical Engineer.